

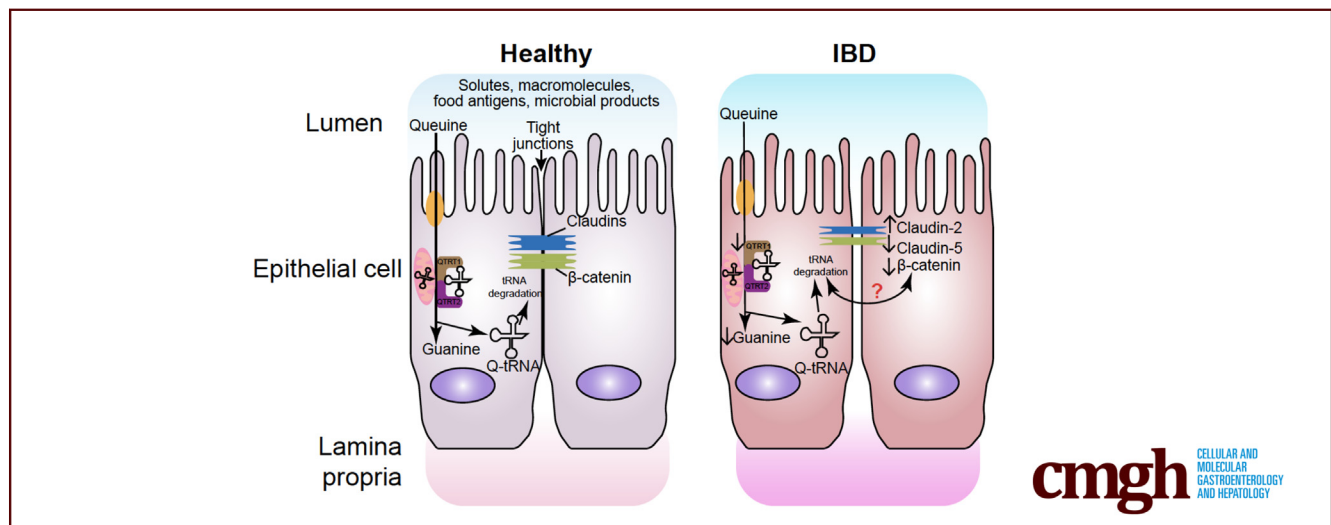
## ORIGINAL RESEARCH

## Disruption to tRNA Modification by Queuine Contributes to Inflammatory Bowel Disease



Jilei Zhang,<sup>1</sup> Yongguo Zhang,<sup>1</sup> Callum J. McGrenaghan,<sup>2</sup> Vincent P. Kelly,<sup>2</sup> Yinglin Xia,<sup>1</sup> and Jun Sun<sup>1,3,4,5</sup>

<sup>1</sup>Division of Gastroenterology and Hepatology, Department of Medicine, University of Illinois Chicago, Chicago, Illinois; <sup>2</sup>School of Biochemistry and Immunology, Trinity Biomedical Sciences Institute, Trinity College, Dublin, Ireland; <sup>3</sup>UIC Cancer Center, Department of Medicine, University of Illinois Chicago, Chicago, Illinois; <sup>4</sup>Department of Microbiology and Immunology, University of Illinois Chicago, Chicago, Illinois; and <sup>5</sup>Jesse Brown VA Medical Center Chicago, Chicago, Illinois



## SUMMARY

Transfer RNA modification determines translation fidelity and efficiency. Human inflammatory bowel disease showed transfer RNA modopathies and altered queuine-related metabolites. QTRT1 (queuine tRNA-ribosyltransferase 1) plays novel functions by altering epithelial cell junctions and proliferation in intestinal inflammation. Queuine protects cells against losing intestinal integrity in inflammation.

**BACKGROUNDS AND AIMS:** Transfer RNA (tRNA) is the most extensively modified RNA in cells. Queuosine modification is a fundamental process for ensuring the fidelity and efficiency of translation from RNA to protein. In eukaryotes, Queuosine tRNA (Q-tRNA) modification relies on the intestinal microbial product queuine. However, the roles and potential mechanisms of Q-containing tRNA (Q-tRNA) modifications in inflammatory bowel disease (IBD) are unknown.

**METHODS:** We explored the Q-tRNA modifications and expression of QTRT1 (queuine tRNA-ribosyltransferase 1) in patients with IBD by investigating human biopsies and reanalyzing datasets. We used colitis models, QTRT1 knockout mice,

organoids, and cultured cells to investigate the molecular mechanisms of Q-tRNA modifications in intestinal inflammation.

**RESULTS:** QTRT1 expression was significantly downregulated in ulcerative colitis and Crohn's disease patients. The 4 Q-tRNA-related tRNA synthetases (asparaginyl-, aspartyl-, histidyl-, and tyrosyl-tRNA synthetase) were decreased in IBD patients. This reduction was further confirmed in a dextran sulfate sodium-induced colitis model and interleukin-10-deficient mice. Reduced QTRT1 was significantly correlated with cell proliferation and intestinal junctions, including downregulation of  $\beta$ -catenin and claudin-5 and the upregulation of claudin-2. These alterations were confirmed *in vitro* by deleting the QTRT1 gene from cells and *in vivo* using QTRT1 knockout mice. Queuine treatment significantly enhanced cell proliferation and junction activity in cell lines and organoids. Queuine treatment also reduced inflammation in epithelial cells. Moreover, altered QTRT1-related metabolites were found in human IBD.

**CONCLUSIONS:** tRNA modifications play an unexplored novel role in the pathogenesis of intestinal inflammation by altering epithelial proliferation and junction formation. Further investigation of the role of tRNA modifications will uncover novel

molecular mechanisms for the prevention and treatment of IBD. (*Cell Mol Gastroenterol Hepatol* 2023;15:1371–1389; <https://doi.org/10.1016/j.jcmgh.2023.02.006>)

**Keywords:** QTRT1; tRNA; IBD; Proliferation; Tight Junctions.

Eukaryotes acquire queuine as a nutrient factor from the intestinal microbiota and the diet. In eubacterial and eukaryotic cells, queuine is found as the sugar nucleotide queuosine at the wobble anticodon position of tRNA for the amino acids tyrosine, histidine, asparagine, and aspartic acid.<sup>1</sup> Queuine produced by the microbiota is taken up from the colonic lumen into enterocytes through cellular uptake mechanisms followed by incorporation into the wobble anticodon position of the 4 tRNAs by a heterodimeric enzyme encoded in the genome.<sup>2–4</sup> This enzyme is composed of a catalytic subunit QTRT1 (queuine tRNA-ribosyltransferase 1) and a noncatalytic partner subunit QTRT2.<sup>5</sup> The physiological requirement for queuine and queuine-modified tRNAs has been broadly documented over 4 decades, establishing relationships to development, proliferation, differentiation, metabolism, cancer, and tyrosine biosynthesis in eukaryotes and invasion in pathogenic bacteria.<sup>2</sup> Starvation for queuine and/or queuosine deficiency in tRNA can cause changes in the pattern of protein synthesis. In addition, queuine deficiency may interfere with other nutrient factors, including vitamin B12, tetrahydrobiopterin, and epidermal growth factor.<sup>1,6</sup> Growing evidence indicates that tRNA modifications play important roles in human diseases (eg, type 2 diabetes).<sup>3</sup> Queuosine depletion led to endoplasmic reticulum stress in mouse liver.<sup>7,8</sup> Queuosine-tRNA (Q-tRNA) modifications are dynamic and highly variable depending on the developmental stages and species type<sup>1,7</sup> and tumorigenesis.<sup>9</sup> However, the health consequences of disturbed availability of queuine and altered Q-tRNA modification remain to be investigated. The effects and mechanisms of Q-tRNA in digestive diseases are unknown.

Inflammatory bowel disease (IBD) is a chronic disease that primarily affects the intestine, including Crohn's disease (CD)<sup>10</sup> and ulcerative colitis (UC). The etiology of IBD has been characterized as chronic intestinal inflammation resulting from many factors, including micronutrients and epigenetic mechanisms via DNA methylation and noncoding RNA.<sup>11,12</sup> Tissue barriers play an essential role in intestinal health.<sup>13</sup> An increase in the tight junction (TJ) protein claudin-2 and a decrease in claudin-5 may lead to the conversion of tight into leaky TJs in IBD patients.<sup>14–18</sup> Our recent study indicated that Q-tRNA modification not only depends on the gut microbiome but also affects TJs, which regulate intestinal permeability in the development of breast cancer.<sup>15</sup> However, the mechanisms by which Q-tRNA modifications are associated with intestinal function in human IBD have never been investigated.

In the current study, we focus on addressing fundamental questions in IBD: is Q-tRNA modification involved in human IBD, and how does dysfunction of Q-tRNA modification contribute to chronic inflammation? We find that


QTRT1 expression is significantly downregulated in UC and CD patients. Four Q-tRNA-related tRNA synthetases (eg, asparaginyl-, aspartyl-, histidyl-, and tyrosyl-tRNA synthetase) were also decreased in IBD patients. Decreased QTRT1 expression was confirmed in experimental dextran sulfate sodium (DSS)-induced colitis and in interleukin (IL)-10-deficient mice. We investigated the impact of QTRT1 on TJs and proliferation in human organoids, cell lines, and colitis models. Insights into Q-tRNA modification in regulating barrier functions will facilitate the development of targeted interventions for IBD through tRNA modifications.

## Results

### Downregulation of QTRT1 in Human IBD Patients

To study the role of Q-tRNA modification, we investigated the expression of QTRT1 in patients with IBD, including both UC and CD patients, and healthy control subjects by revisiting datasets in the National Center for Biotechnology Information Gene Expression Omnibus (GEO) database (<https://www.ncbi.nlm.nih.gov/geo>). In the dataset with accession number GSE9452,<sup>19</sup> biopsies from the descending colon were collected from 14 UC patients with macroscopic signs of inflammation and 5 patients without any inflammation signs. We found that the messenger RNA (mRNA) expression of QTRT1, the critical catalytic subunit Q-tRNA modification, was significantly downregulated in the intestinal mucosa of the patients with UC symptoms compared with the non-UC patients ( $P = .05$ ) (Figure 1A). Similarly, when we reanalyzed the GSE83448 dataset,<sup>20</sup> which has ileal biopsy samples from 39 patients with CD symptoms and 14 patients without any intestinal symptoms, QTRT1 expression was also found to be significantly downregulated in CD patients compared with control subjects ( $P = .01$ ) (Figure 1B). Because these downregulations were found at the mRNA level, we further investigated the alterations of QTRT1 protein expression in the biopsy colon tissue from IBD patients by immunohistochemistry (IHC) staining. In the UC patients, the QTRT1 staining intensity in the intestinal biopsy tissue was significantly reduced compared with control subjects ( $P = .01$ ) (Figure 1C). Meanwhile, the expression of QTRT1 was also found to be significantly downregulated in the intestinal tissue of CD patients compared with normal control subjects ( $P = .01$ ). However, no staining was observed in our IgG negative control for IHC staining (Figure 1D). More importantly, our

**Abbreviations used in this paper:** CD, Crohn's disease; DSS, dextran sulfate sodium; eTGT, eukaryotic transfer RNA-guanine transglycosylase; GEO, Gene Expression Omnibus; IBD, inflammatory bowel disease; IF, immunofluorescence; IHC, immunohistochemistry; IL, interleukin; mRNA, messenger RNA; PCNA, proliferating cell nuclear antigen; PCR, polymerase chain reaction; Q-tRNA, queuosine-containing transfer RNA; TEER, transepithelial electrical resistance; tRNA, transfer RNA; TJ, tight junction; UC, ulcerative colitis.

 Most current article

© 2023 The Authors. Published by Elsevier Inc. on behalf of the AGA Institute. This is an open access article under the CC BY-NC-ND license (<http://creativecommons.org/licenses/by-nc-nd/4.0/>).

2352-345X

<https://doi.org/10.1016/j.jcmgh.2023.02.006>

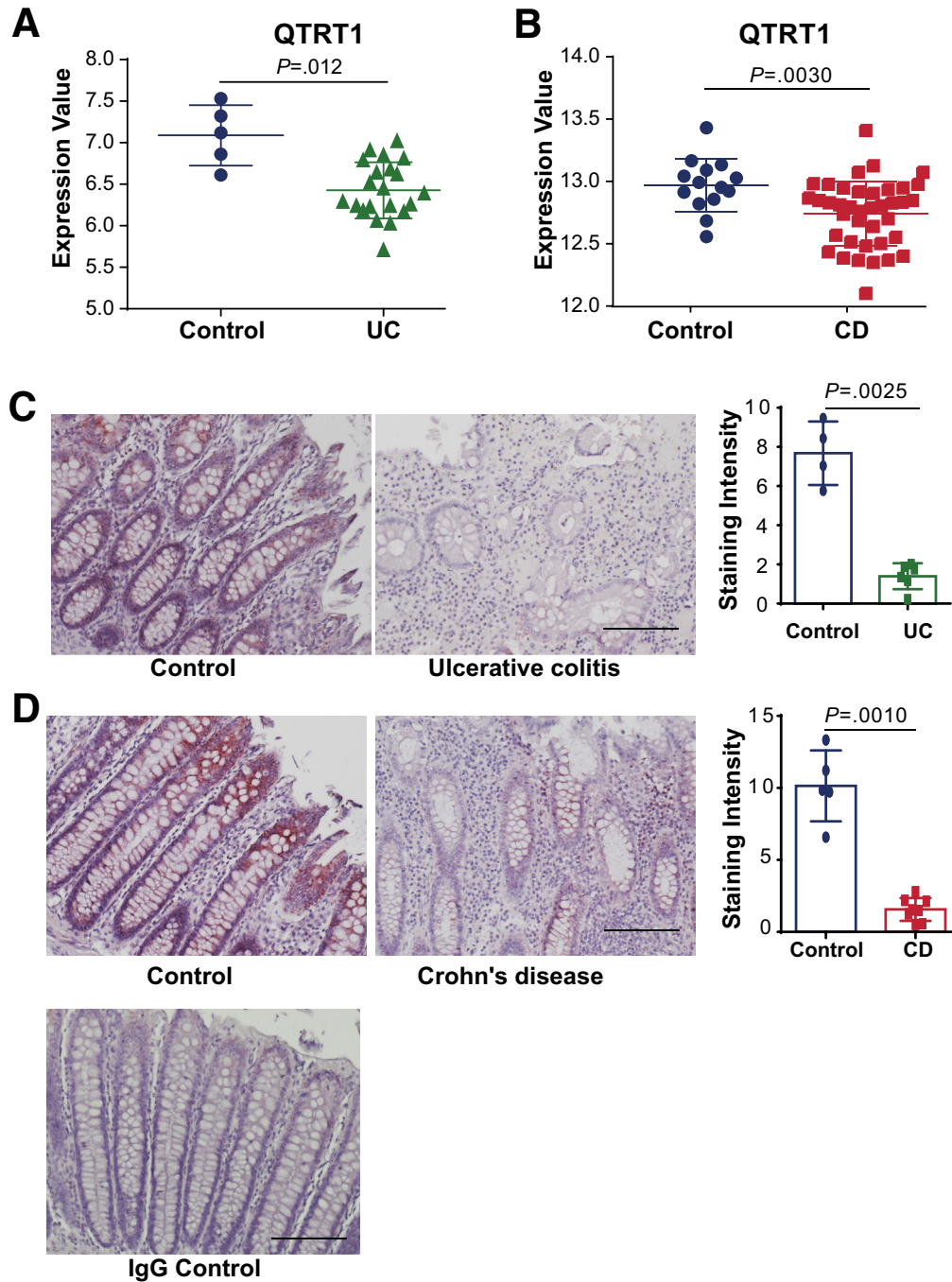


**Figure 1. Expression of QTRT1 in human CD and UC patients.** (A) Graphs of RNA-sequencing gene expression levels of QTRT1 in human colon biopsies of UC patients ( $n = 21$ ) and control subjects ( $n = 5$ ) from published databases. The data of UC patients were from National Center for Biotechnology Information GEO datasets with accession number GSE9452. Data are shown as mean  $\pm$  SD, Welch's  $t$  test. (B) Graphs of RNA-sequencing gene expression levels of QTRT1 in human colon biopsies of CD patients ( $n = 39$ ) and control subjects ( $n = 14$ ) from published databases. The data of CD patients were from National Center for Biotechnology Information GEO datasets with accession number GSE83448. Data are shown as mean  $\pm$  SD, Welch's  $t$  test. (C) Representative IHC staining of QTRT1 in colon tissue from UC patients ( $n = 6$ ) and control subjects ( $n = 4$ ). The scale bar is  $300 \mu\text{m}$ . Semiquantitative analysis was performed on IHC staining using ImageJ Fiji. Data are shown as mean  $\pm$  SD, Welch's  $t$  test. (D) Representative IHC staining of QTRT1 in colon tissue from CD patients ( $n = 8$ ) and control subjects ( $n = 5$ ). The scale bar is  $300 \mu\text{m}$ . Semiquantitative analysis was performed on IHC staining using ImageJ Fiji. Data are shown as mean  $\pm$  SD, Welch's  $t$  test. IgG was used as a negative control for all IHC staining.

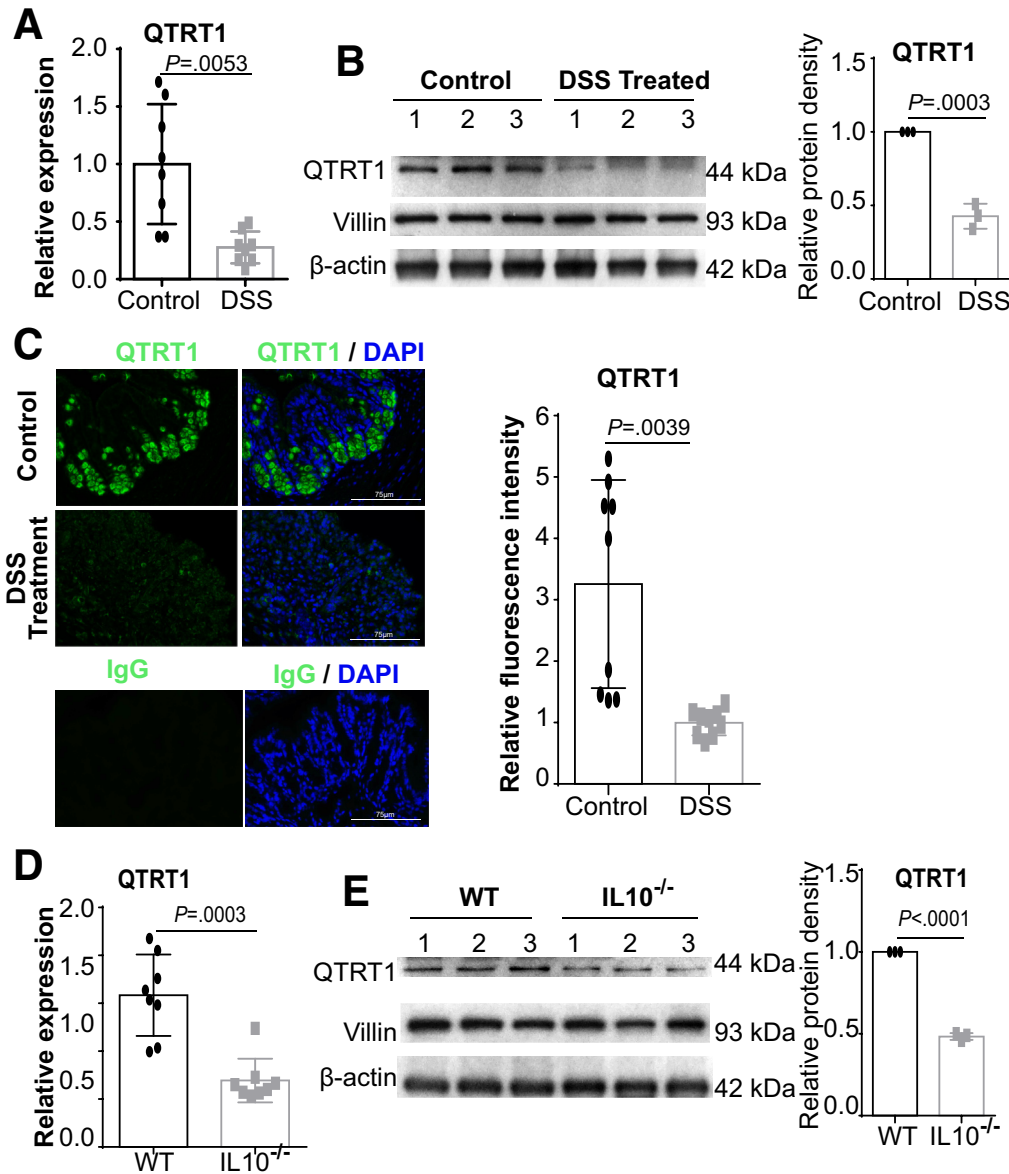


**Figure 2. Expression of QTRT1 and junction proteins in the IBD mouse model.** (A) mRNA expression of QTRT1 in DSS-induced colitis mice. Data are expressed as mean  $\pm$  SD, Welch's *t* test. *n* = 4 (one-repeat well) mice per group. (B) QTRT1 protein expression levels were evaluated in the intestinal epithelial cells of mice treated with DSS and control animals using Western blotting. Data are expressed as mean  $\pm$  SD, Welch's *t* test. *n* = 3 mice per group. (C) QTRT1 expression in colons from DSS-treated mice was visualized by IF staining. Mouse IgG was used as the negative experimental control in all the staining. The scale bar is 75  $\mu$ m. The relative fluorescence intensity was quantified with ImageJ by counting 3 images for each sample. Data are shown as mean  $\pm$  SD, Welch's *t* test. *n* = 3 per group. (D) mRNA expression of QTRT1 in IL-10 knockout mice. Data are expressed as mean  $\pm$  SD, Welch's *t* test. *n* = 4 (one-repeat well) mice per group. (E) QTRT1 protein levels were evaluated in the intestinal epithelial cells of IL10<sup>-/-</sup> mice and WT mice using Western blotting. Data are expressed as mean  $\pm$  SD, Welch's *t* test. *n* = 3 mice per group.

findings of QTRT1 alteration at the protein level were consistent with the mRNA level in IBD patients. Taken together, we found that QTRT1 was downregulated at the mRNA and protein levels in the intestinal mucosa of IBD patients, including UC and CD patients.

#### Reduction of QTRT1 in Colitis Mouse Models

We then further investigated the expression of QTRT1 in colonic cells from IBD mouse models, including a

DSS-induced colitis mouse model and an IL-10-deficient mouse model (Figure 2). We first evaluated the mRNA expression of QTRT1 in colon tissue using real-time polymerase chain reaction (PCR). We found that the mRNA expression of QTRT1 was significantly downregulated in the colon tissue from the DSS-treated mice compared with the nontreated control mice ( $P = .01$ ) (Figure 2A). Then, we evaluated the protein expression of QTRT1 in the colon tissue of DSS-induced colitis mice via Western blot analysis. Clearly, the expression of QTRT1 in the DSS-treated mice

was significantly suppressed compared with that of control subjects ( $P = .001$ ) (Figure 2B). To further verify the protein expression of QTRT1 in the colitis mouse model, immunofluorescence (IF) staining was performed on colon tissue collected from DSS-treated mice. Inflammation and intestinal damage were found in the colon tissue from the DSS-treated mice (Figure 2C). Additionally, the expression of QTRT1 (fluorescence intensity) in the mice with colitis was significantly suppressed compared with that of nontreated control mice ( $P = .01$ ) (Figure 2C). However, there was no fluorescence staining in the IgG negative control used in the whole process of IF staining.

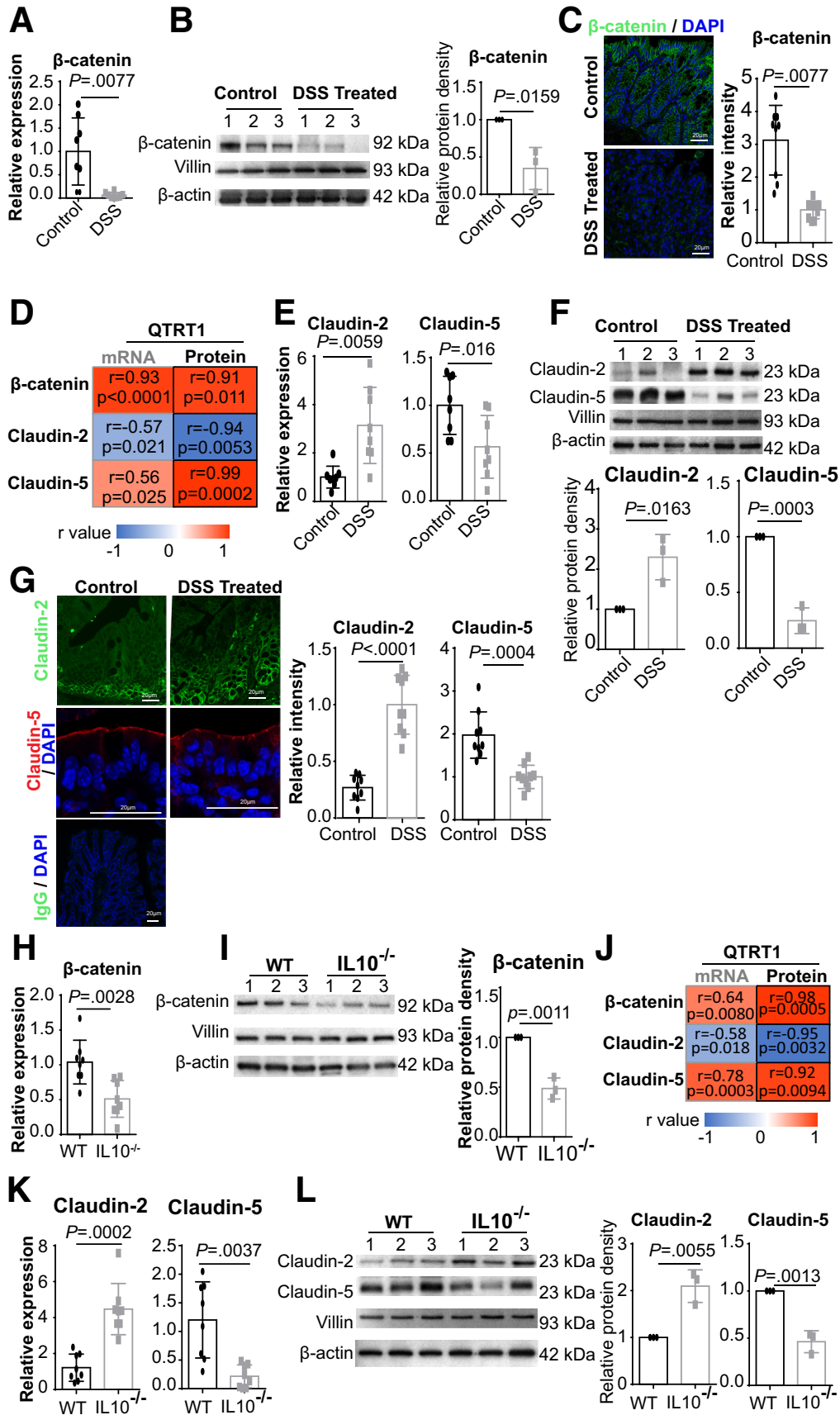
Among the most used IBD models, IL-10-deficient mice (IL-10<sup>-/-</sup>) spontaneously develop chronic enterocolitis.<sup>21,22</sup> This spontaneous onset of gut inflammation (colitis) in IL-10-deficient mice is characterized by histological findings that reflect those of human IBD.<sup>23</sup> Here, we further investigated the Q-tRNA modification, mainly QTRT1 expression, in the colon of IL-10-deficient mice with inflammation. After colonic epithelial cell collection and total RNA extraction, we detected the mRNA level of QTRT1 using real-time PCR. Similar to the results we found in DSS-induced colitis, QTRT1 expression in IL-10<sup>-/-</sup> mice was significantly suppressed compared with that of wild-type (WT) mice ( $P = .001$ ) (Figure 2D). Furthermore, we performed Western blot analysis to evaluate the protein expression level and detected significantly reduced expression of QTRT1 in IL-10<sup>-/-</sup> mice compared with WT mice ( $P = .001$ ) (Figure 2E). Taken together, QTRT1 expression is significantly reduced in DSS-induced colitis and IL10<sup>-/-</sup> mouse models, suggesting dysfunction of queuosine modification in the inflamed intestine.

### Reduced QTRT1 Is Associated With Altered $\beta$ -Catenin and Claudins in Colitis Mouse Models

To investigate how regulatory genes are affected by the downregulation of QTRT1 in intestinal inflammation, we evaluated the expression of adhesion molecules and TJ regulators in colitis mouse models.  $\beta$ -catenin is an evolutionarily conserved, multifunctional protein with a crucial role in development and homeostatic processes, such as cell proliferation and adhesion.<sup>24</sup> We found significantly downregulated expression of  $\beta$ -catenin at the mRNA level in colon tissue from DSS-treated mice compared with nontreated mice ( $P = .01$ ) (Figure 3A). Meanwhile, the protein expression of  $\beta$ -catenin was also significantly downregulated in the colon of DSS-treated mice ( $P = .05$ ) (Figure 3B). Importantly, we found a significantly positive correlation of the QTRT1 alteration (Figure 2) and  $\beta$ -catenin alteration at both the mRNA (correlation = 0.93,  $P = 1.1 \times 10^{-7}$ ) and protein level (correlation = 0.91,  $P = .011$ ) using the Spearman correlation test (Figure 3D). Furthermore, IF staining of  $\beta$ -catenin was applied to colon tissue to verify the changes in  $\beta$ -catenin, which was significantly downregulated (fluorescence intensity) in mice with colitis ( $P = .01$ ) (Figure 3C). All these findings highlighted the critical role of Q-tRNA modification in  $\beta$ -catenin-related cell proliferation and colitis.

TJs are intercellular adhesion complexes in intestinal epithelia and endothelia that control paracellular permeability. Claudins are a family of transmembrane barrier proteins that form paracellular gated ion-selective pores, with claudin-5 being responsible for the watertight barrier of the cell and claudin-2 being permeable to both ions and water,<sup>25</sup> thus ensuring proper availability of water and ions for effective cellular function. Here, in our DSS-induced colitis mouse model, significant upregulation of mRNA expression of claudin-2 ( $P = .01$ ) and significant downregulation of claudin-5 ( $P = .05$ ) were observed in the colon of DSS-treated mice compared with nontreated mice (Figure 3E). Consistent with the reduction in mRNA, Western blotting showed that claudin-2 was significantly upregulated ( $P = .05$ ) and that claudin-5 was significantly downregulated ( $P = .001$ ) in diseased animals relative to control animals (Figure 3F). Using the Spearman correlation test, we found that these protein alterations in Claudin-2 (correlation = -0.94,  $P = .0053$ ) and claudin-5 (correlation = 0.99,  $P = .00017$ ) were significantly correlated with the protein alteration of QTRT1 (Figure 2) in DSS-treated mice and control mice (Figure 3D). Moreover, we further examined the alterations in claudin-2 and claudin-5 using IF staining and found that the fluorescence was significantly upregulated for claudin-2 ( $P = .001$ ) and downregulated for claudin-5 ( $P = .001$ ) (Figure 3G). However, there was no fluorescence staining in the IgG negative control used in the whole process of IF staining described in this section. Furthermore, we found that these alterations correlate with QTRT1 downregulation.

We then investigated the correlation of QTRT1 regulation with cell proliferation and the function of intestinal junctions in IL-10-deficient mice. First, we evaluated the mRNA expression of  $\beta$ -catenin using real-time PCR, in which we found significant downregulation of  $\beta$ -catenin compared with that of WT mice ( $P = .05$ ) (Figure 3H). These changes in  $\beta$ -catenin were also verified at the protein level by Western blot analysis using IL-10-deficient mice and WT mice ( $P = .001$ ) (Figure 3I). Moreover, these protein alterations in  $\beta$ -catenin in IL-10 deficient mice significantly correlated with the downregulation of QTRT1 (Figure 2) for both mRNA (correlation = 0.64,  $P = .0080$ ) and protein (correlation = 0.98,  $P = .00050$ ) using Spearman correlation test (Figure 3J). Next, we evaluated the mRNA expression of claudin-2 and claudin-5 in IL-10-deficient mice using real-time PCR as described above. Similar to the results we found in the DSS-induced colitis model, there was a significant upregulation of claudin-2 mRNA expression ( $P = .01$ ) and a downregulation of claudin-5 ( $P = .01$ ) in IL-10-deficient mice (Figure 3K). Using Western blotting, we then investigated the protein expression levels of the target genes and found a significant upregulation of claudin-2 ( $P = .01$ ) and a downregulation of claudin-5 ( $P = .01$ ) in the colon tissue of IL-10-deficient mice when compared with WT control subjects (Figure 3L). Moreover, we found the alterations of claudin-2/claudin-5 significantly correlate with the changes in QTRT1 at both mRNA (claudin-2: correlation = -0.58,  $P = .018$ ; claudin-5: correlation = 0.78,  $P = .00034$ ) and protein (claudin-2: correlation = -0.95,  $P =$



.0032; claudin-5: correlation = 0.92,  $P = .0094$ ) levels (Figure 3J). Taken together, we find a clear correlation between the downregulation of  $\beta$ -catenin and claudin-5 and the upregulation of claudin-2 with the downregulation of QTRT1 in the inflamed colon of DSS-treated and IL-10-deficient mice (Figure 3). These findings highlight the importance of QTRT1 in cellular proliferation and intestinal barrier function *in vivo*.

### Reduced QTRT1 Is Associated With Altered Adhesion and Junctions In Vitro and In Vivo

Because of the critical role of QTRT1 in the inflamed intestine in our *in vivo* mouse models, we next investigated the impact of QTRT1 suppression on cell function *in vitro*. Using a loss-of-function study, we suppressed the expression of QTRT1 to investigate its regulatory role in cell proliferation and junction proteins. To this end, we suppressed the expression of QTRT1 in Caco2 BBE cells using a double nickase plasmid, which resulted in a significant downregulation of QTRT1 expression at both the mRNA and protein levels (Figure 4). Cellular proliferation was significantly suppressed by the knockdown<sup>26</sup> of QTRT1 in Caco2 BBE cells, indicated by the downregulation of proliferating cell nuclear antigen (PCNA) expression in the knockdown cells, relative to control cells (Figure 4A and B). Meanwhile, the expression of adhesion and TJ proteins, including  $\beta$ -catenin, claudin-2 and claudin-5, was also changed in QTRT1 knockdown cells, which were consistent with the previous *in vivo* findings. Using real-time PCR, Western blotting, and IF staining, we found that  $\beta$ -catenin and claudin-5 expression was significantly downregulated in QTRT1 knockdown cells compared with control Caco2 BBE cells at both the mRNA ( $P = .05$ ) (Figure 4A) and protein ( $P = .001$ ) levels (Figure 4B and C). However, the knockdown of QTRT1 significantly upregulated the expression of claudin-2 in the QTRT1 knockdown Caco2 BBE cells at both the mRNA ( $P = .01$ ) (Figure 4A) and protein ( $P = .01$ ) levels

(Figure 4B). There was no observable fluorescence staining in the IgG negative control used in the whole process of the IF staining described in this section.

To further verify our findings on the influence of QTRT1 knockdown on cell proliferation and junction activity, we evaluated the mRNA and protein expression of  $\beta$ -catenin and claudins in human HCT116 colon epithelial cells. The significantly downregulated mRNA expression (Figure 4D) and protein expression (Figure 4E) of QTRT1 in the HCT116 knockdown cells clearly showed the knockdown of QTRT1 in these cells. Cell proliferation was suppressed after knockdown of QTRT1, as indicated by the downregulation of PCNA expression (Figure 4D and E). Similar to previous findings, we found  $\beta$ -catenin and claudin-5 to be downregulated and claudin-2 upregulated in QTRT1 knockdown HCT116 cells, compared with control cells (Figure 4D and E). Taken together, these findings clearly show the impact of QTRT1 knockdown on cell proliferation and junctions by altering the expression of PCNA,  $\beta$ -catenin, and claudins in 2 human intestinal epithelial cell lines.

We also used the QTRT1 knockout mice to further confirm our findings in cells. Compared with WT animals, knockout mice showed a significant downregulation in  $\beta$ -catenin and claudin-5 expression by both Western blot and IF staining (Figure 5).

### Alteration of QTRT1-Related Metabolites

The guanine is exchanged from the tRNA-containing guanosine with queuine to obtain Q-tRNA, whose reaction is controlled by the eukaryotic tRNA-guanine transglycosylase (eTGT) composed of QTRT1 and QTRT2 subunits. Therefore, the dysfunction of QTRT1, the catalytic subunit of eTGT, in IBD patients may further influence the abundance of metabolites related to QTRT1-regulated pathways. Thereafter, the abundance of guanine in the feces was compared between IBD patients and control subjects by revisiting metabolite data from the

**Figure 3. Expression of  $\beta$ -catenin and claudin proteins in colitis mice and control animals.** (A) mRNA expression of  $\beta$ -catenin in DSS-induced colitis mice. Data are expressed as mean  $\pm$  SD, Welch's  $t$  test.  $n = 4$  (one-repeat well) mice per group. (B)  $\beta$ -Catenin protein expression levels were evaluated in the intestinal epithelial cells of mice treated with DSS and control subjects by Western blotting. Data are expressed as mean  $\pm$  SD, Welch's  $t$  test.  $n = 3$  mice per group. (C)  $\beta$ -catenin expression in colons from DSS-treated mice were visualized by IF staining. The scale bar is 20  $\mu$ m. The relative fluorescence intensity was quantified using ImageJ by counting 3 images for each sample. Data are shown as mean  $\pm$  SD, Welch's  $t$  test.  $n = 3$  per group. (D) The correlation of QTRT1 alteration in Figure 2 and alterations of  $\beta$ -catenin and claudins was analyzed for mRNA (real-time PCR) and protein (Western blot) levels using Spearman's rank correlation coefficient. The correlation coefficient value  $r$  and  $P$  value were indicated in the frames and color bar. (E) mRNA expression of claudin-2 and claudin-5 in DSS-induced colitis and control mice. Data are expressed as mean  $\pm$  SD, Welch's  $t$  test.  $n = 4$  (one-repeat well) mice per group. (F) claudin protein levels were evaluated in the intestinal epithelial cells of DSS-treated mice and control mice using Western blotting. Data are expressed as mean  $\pm$  SD, Welch's  $t$  test.  $n = 3$  mice per group. (G) Claudins in the colon from DSS-treated mice were visualized by IF staining. The scale bar is 20  $\mu$ m. The relative fluorescence intensity was quantified using ImageJ by counting 3 images for each sample. Data are shown as mean  $\pm$  SD, Welch's  $t$  test.  $n = 3$  per group. IgG was used as the negative experimental control in all IF staining. (H) mRNA expression of  $\beta$ -catenin in IL-10 knockout and WT mice. Data are expressed as mean  $\pm$  SD, Welch's  $t$  test.  $n = 4$  (one-repeat well) mice per group. (I)  $\beta$ -Catenin protein expression levels were evaluated in the intestinal epithelial cells of IL-10 knockout and WT mice using Western blotting. Data are expressed as mean  $\pm$  SD, Welch's  $t$  test.  $n = 3$  mice per group. (J) The correlation of QTRT1 alteration in Fig 2. and alterations of  $\beta$ -catenin and claudins was analyzed for mRNA (real-time PCR) and protein (Western blot) levels using Spearman's rank correlation coefficient. The correlation coefficient value  $r$  and  $P$  value were indicated in the frames and color bar. (K) mRNA expression of claudin-2 and claudin-5 in IL-10 knockout and WT mice. Data are expressed as mean  $\pm$  SD, Welch's  $t$  test.  $n = 4$  (one-repeat well) mice per group. (L) Claudin protein levels were evaluated in the intestinal epithelial cells of IL-10 knockout and WT mice using Western blotting. Data are expressed as mean  $\pm$  SD, Welch's  $t$  test.  $n = 3$  mice per group.

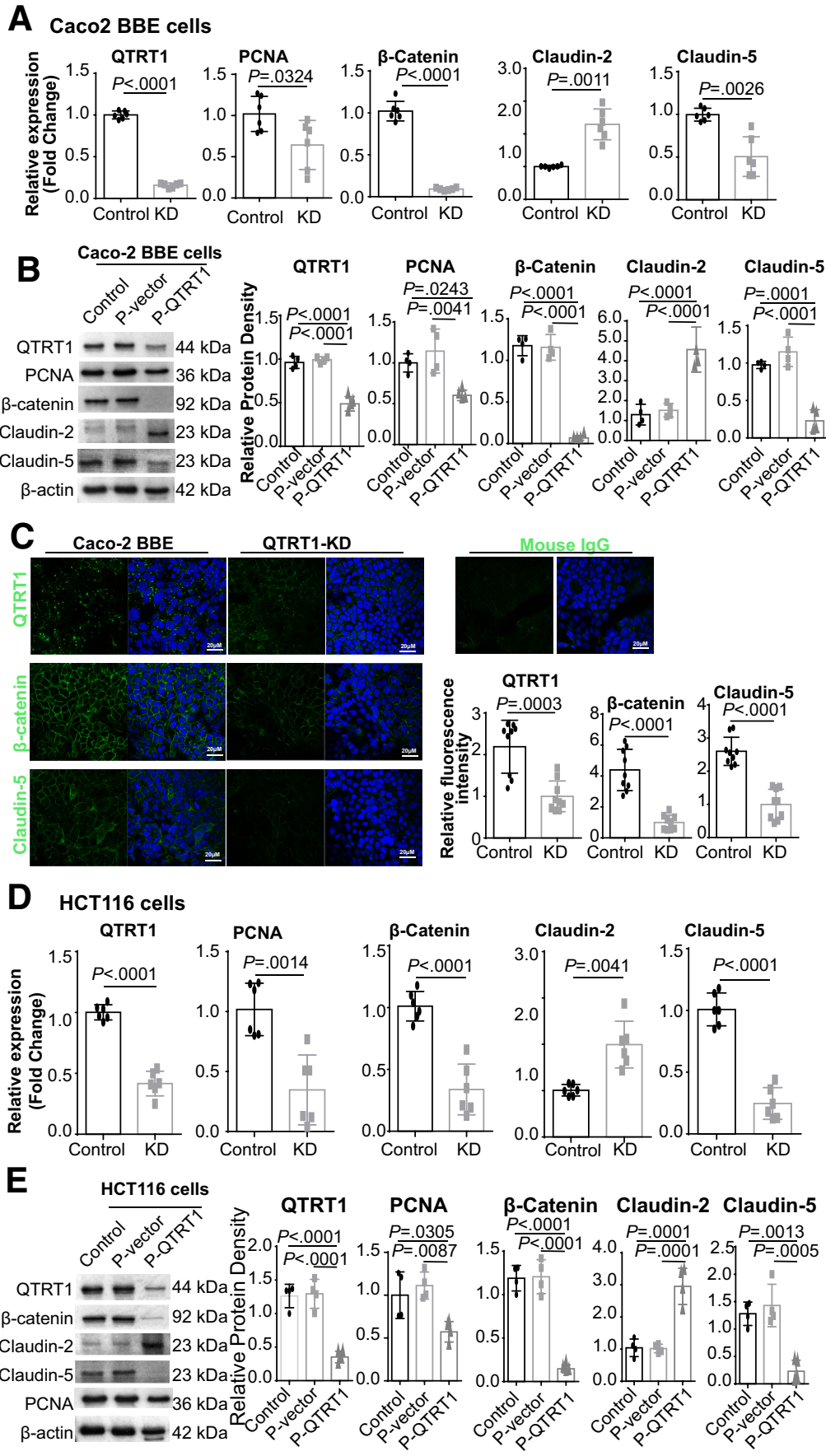


**Figure 4. Expression of  $\beta$ -catenin and claudins in QTRT1 knockdown (KD) cells.** (A) The mRNA expression levels of targeted genes in Caco-2 BBE cells, including QTRT1 KD<sup>26</sup> by transfection with QTRT1 double nickase plasmid and control subjects, were measured by real-time PCR. Data are expressed as mean  $\pm$  SD, Welch's *t* test. *n* = 3 (one-repeat well) per group. (B) Protein expression of targeted genes in Caco2 cells transfected with QTRT1 double nickase plasmid or control double nickase plasmids (P-vector) and negative control was evaluated by Western blotting. Data are expressed as mean  $\pm$  SD, one-way analysis of variance. *n* = 4 per group. (C) Targeted protein expression in QTRT1 KD Caco-2 BBE cells was visualized by IF staining. The scale bar is 20  $\mu$ m. The relative fluorescence intensity was quantified using ImageJ by counting 3 images for each sample. Data are shown as mean  $\pm$  SD, Welch's *t* test. *n* = 3 per group. (D) The mRNA expression levels of targeted genes in HCT116 cells, including QTRT1 KD<sup>26</sup> by transfection with QTRT1 double nickase plasmid (h) and control subjects, were measured by real-time PCR. Data are expressed as mean  $\pm$  SD, Welch's *t* test. *n* = 3 (one-repeat well) per group. (E) Protein expression of targeted genes in CHT116 cells transfected with QTRT1 double nickase plasmid (h) or P-vector and negative control was evaluated by Western blotting. Data are expressed as mean  $\pm$  SD, one-way analysis of variance. *n* = 4 per group.



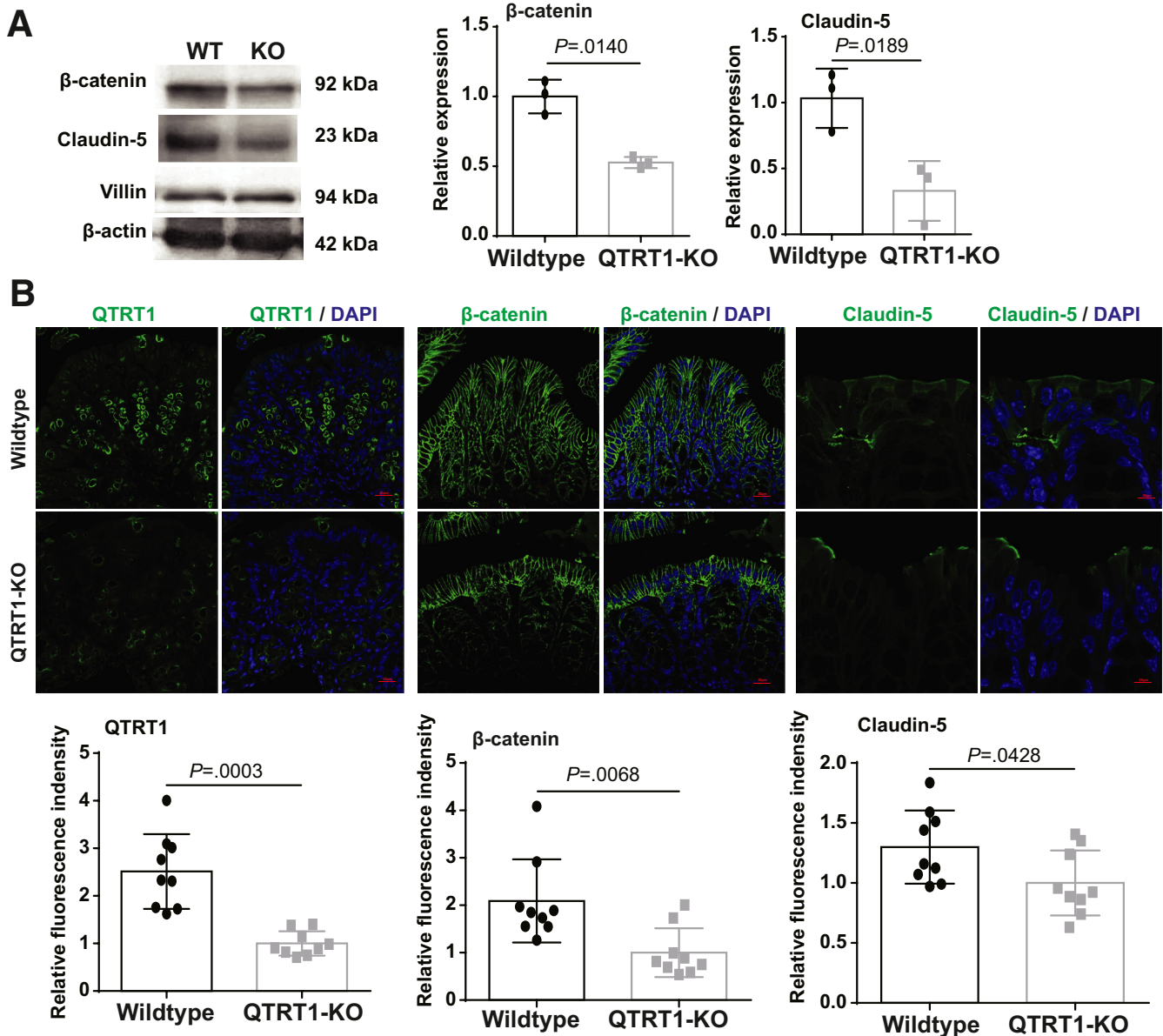


**Figure 5. Expression of  $\beta$ -catenin and claudins in QTRT1 knockout (KO) mice.** (A) Protein expression of targeted genes in colon from QTRT1 KO and WT mice was evaluated by Western blotting. Data are expressed as mean  $\pm$  SD, Welch's *t* test. *n* = 3 per group. (B) Targeted protein expression in principal colon from QTRT1 KO and WT mice was visualized by IF staining. The scale bar is 20  $\mu$ m. The relative fluorescence intensity was quantified using ImageJ by counting 3 images for each sample. Data are shown as mean  $\pm$  SD, Welch's *t* test. *n* = 3 per group.

Metabolomics Workbench (<https://www.metabolomicsworkbench.org/>).

There are 2 datasets of IBD research: the project PR000639 with 145 UC patients, 266 CD patients, and 134 control subjects without any IBD symptoms<sup>27</sup>; and the project PR000677 with 76 UC patients, 88 CD patients, and 56 control subjects without any IBD symptoms.<sup>28</sup> For the UC patients, the abundance of guanine was significantly downregulated compared with control subjects in both projects ( $P = .001$  and  $P = .05$ , respectively) (Figure 6A). Similarly, guanine abundance in the feces of patients with CD symptoms was significantly downregulated compared with control subjects without CD symptoms in both projects

used in this study ( $P = .001$  and  $P = .05$ , respectively) (Figure 6B).

In eubacteria and eukaryotes, queuine is found as the sugar nucleotide queuosine within the anticodon loop of tRNA isoacceptors for the amino acids tyrosine, asparagine, aspartic acid, and histidine.<sup>1</sup> Because of the dysfunction of QTRT1 and alteration of guanine in IBD patients, it is reasonable to hypothesize that the changed Q-tRNA in IBD patients further alters the related tRNA synthetases. Therefore, we investigated the synthetase expression level of these 4 tRNAs, which are related to Q-tRNA modification, in both UC and CD patients and normal control subjects from the available datasets. We found that 3 tRNA synthetases, asparaginyl-tRNA

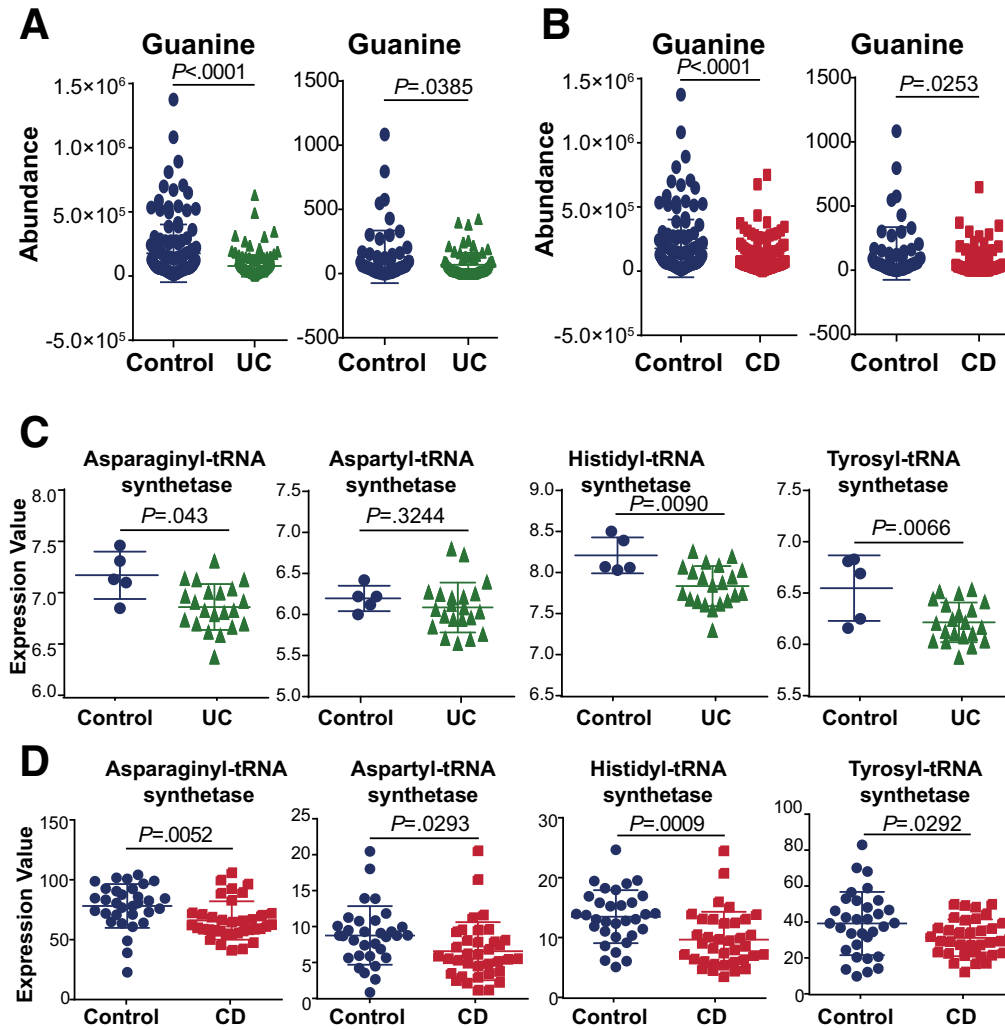


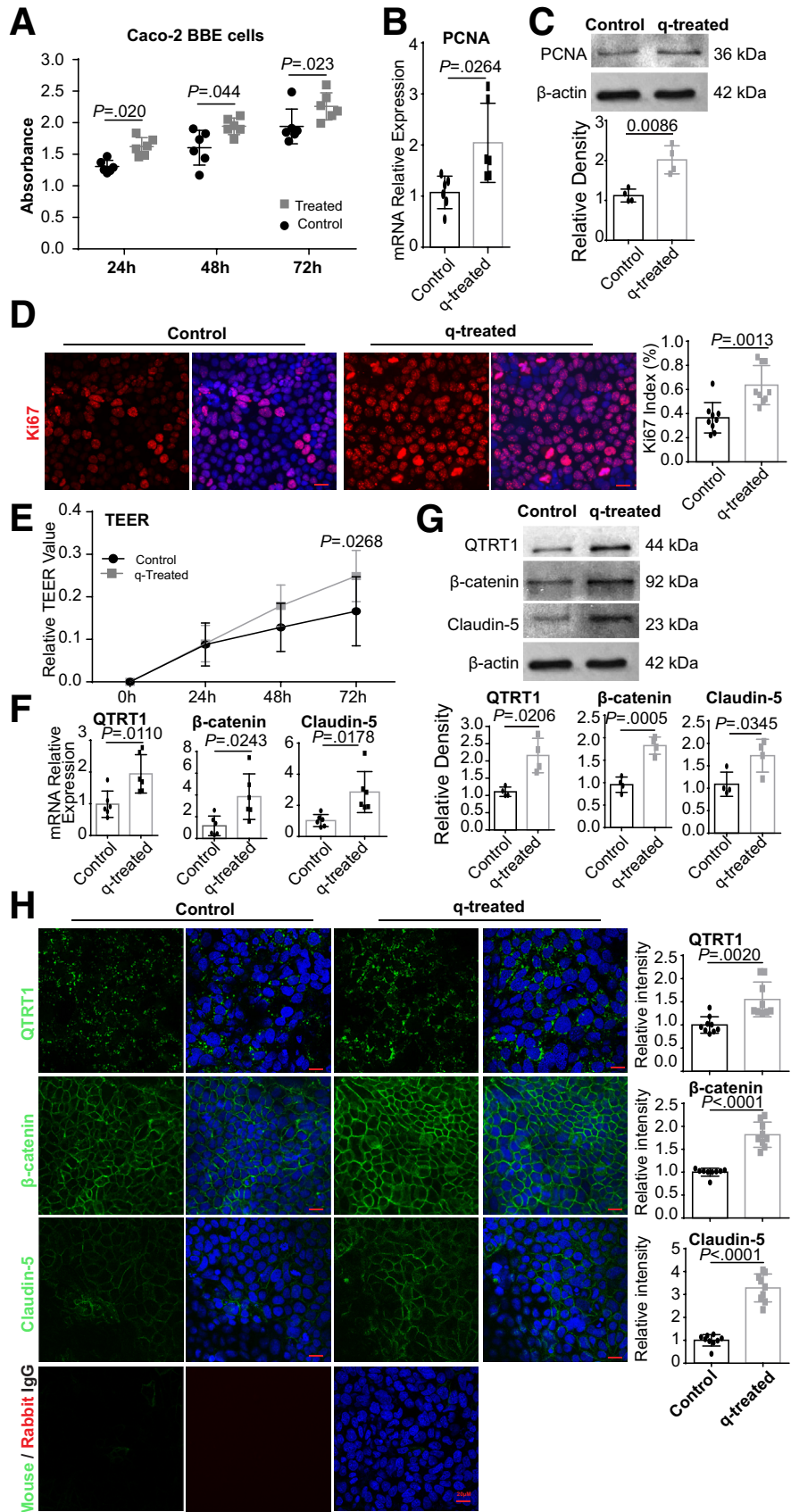
**Figure 6.** Alterations of metabolites related to QTRT1 in human IBD patients. In tRNA containing a GUN anticodon (where N = any base), guanine at position 34 is exchanged with queuine to obtain queuosine-modified tRNA, a reaction carried out by the eTGT enzyme, which is composed of subunits of QTRT1 and QTRT2 subunits. The abundance of guanine was compared between IBD patients and control subjects by revisiting metabolite data from Metabolomics Workbench. Alteration of guanine in (A) UC and (B) CD patients. Two datasets were included in the analysis with project numbers PR000639 (UC: n = 145; CD: n = 266; control: n = 134) and PR000677 (UC: n = 76; CD: n = 88; control: n = 56). The data are shown as mean  $\pm$  SD, Welch's *t* test. (C) The abundance of the 4 tRNA synthetases that are modified with queuine (asparaginyl, aspartyl, histidyl, and tyrosyl) was compared in UC patients (n = 14) and control subjects (n = 5) sourced from GEO datasets with accession number GSE9452. (D) Four synthetases of tRNAs (asparaginyl, aspartyl, histidyl, tyrosyl) were compared between CD patients (n = 36) and control subjects (n = 32) sourced from ArrayExpress with accession number E-MTAB-5783. The data are shown as mean  $\pm$  SD, Welch's *t* test.

synthetase ( $P = .05$ ), histidyl-tRNA ( $P = .01$ ) and tyrosyl-tRNA synthetase ( $P = .01$ ), were significantly downregulated in the intestinal mucosa of UC patients (n = 14) compared with control subjects (n = 5) from GSE9442 (Figure 6C). Although there were no significant differences in aspartyl-tRNA synthetase between UC patients and control subjects ( $P = .32$ ), a trend of downregulation was observed (Figure 6C). Meanwhile, all 4 tRNA synthetases, including asparaginyl tRNA synthetase ( $P = .01$ ), aspartyl-tRNA synthetase ( $P = .05$ ), histidyl-tRNA ( $P = .001$ ), and tyrosyl-tRNA synthetase ( $P = .05$ ), were significantly downregulated in the intestinal mucosa of CD patients (n = 36) compared with control subjects (n = 32) (Figure 6D).

### Queuine Treatment Enhances the Proliferation and TJs of Epithelial Cells In Vitro

To further evaluate the critical role of QTRT1 and related molecules in cell biosynthesis, we treated Caco-2 BBE cells with queuine, which is the substrate of the biosynthesis of Q-tRNA. As we found previously that QTRT1 deletion markedly impacted cell proliferation, we measured the cell proliferation activity of the cells using MTT assay. The cell proliferation activity was significantly ( $P = .05$ ) upregulated after 24 hours of treatment with queuine, compared with that in untreated cells. This upregulation lasted from 48 hours to 72 hours post-treatment (Figure 7A). This upregulated cell proliferation was further verified by the

**Figure 7. Queuine treatment regulates cell proliferation and permeability.** (A) An MTT assay showing the proliferation of control and Caco-2 BBE cells treated with queuine hydrochloride was conducted at 24, 48, and 72 hours after treatment. Data are expressed as mean  $\pm$  SD, generalized linear mixed models.  $n = 6$  per group. (B) The mRNA expression level of PCNA in Caco-2 BBE cells treated with queuine for 72 hours were measured by real-time PCR. Data are expressed as mean  $\pm$  SD, Welch's  $t$  test.  $n = 3$  (one-repeat well) per group. (C) The protein expression of PCNA in Caco-2 BBE cells treated with queuine for 72 hours was measured by Western blotting. Data are expressed as mean  $\pm$  SD, Welch's  $t$  test.  $n = 3$  per group. (D) Immunofluorescence staining of the cell proliferation marker Ki67 was performed in Caco-2 BBE cells after 72 hours of queuine treatment. The Ki67 index was calculated with the formula: Ki67-positive cells/total cells. The relative fluorescence intensity was quantified using ImageJ by counting 3 images for each sample. Data are expressed as mean  $\pm$  SD, Welch's  $t$  test.  $n = 3$  per group. (E) The TEER value was measured and monitored on HT-29 cells at 24, 48, and 72 hours after treatment with queuine. Data were expressed as mean  $\pm$  SD, two-way analysis of variance.  $n = 6$  per group. (F) The mRNA expression levels of QTRT1,  $\beta$ -catenin, and claudin-5 in Caco-2 BBE cells treated with queuine for 72 hours were measured by real-time PCR. Data are expressed as mean  $\pm$  SD, Welch's  $t$  test.  $n = 3$  (one-repeat well) per group. (G) The protein expression of QTRT1,  $\beta$ -catenin, and claudin-5 in Caco-2 BBE cells treated with queuine for 72 hours was measured by Western blotting. Data are expressed as mean  $\pm$  SD, Welch's  $t$  test.  $n = 3$  per group. (H) IF staining of the cell proliferation markers QTRT1,  $\beta$ -catenin, and claudin-5 was performed in Caco-2 BBE cells after 72 hours of queuine treatment. The relative fluorescence intensity was quantified using ImageJ by counting 3 images from each sample. Data are expressed as mean  $\pm$  SD, Welch's  $t$  test.  $n = 3$  per group.



increased expression of the cell proliferation marker PCNA using real-time PCR ( $P = .05$ ) (Figure 7B). We also verified the upregulation of PCNA using Western blot analysis, which showed significantly higher expression compared with control subjects ( $P = .01$ ) (Figure 7C). Using IF staining of Ki67, another cell proliferation marker, we found a significantly higher Ki67-positive cell ratio in queuine-treated Caco2 BBE cells than in control cells ( $P = .01$ ) (Figure 7D), indicating high cell proliferation activities in queuine-treated cells.

Subsequently, we investigated the impact of queuine treatment on cell permeability *in vitro*. Using the trans-epithelial electrical resistance (TEER) assay, we found a significantly higher TEER value after treating the cells for 72 hours with queuine ( $P = .05$ ) (Figure 7E). These altered cell permeability and cell proliferation benefited from the upregulated expression of QTRT1 in the queuine-treated cells, which was indicated at both the mRNA level by real-time PCR ( $P = .05$ ) (Figure 7F) and the protein level by Western blot ( $P = .05$ ) (Figure 7G), which indicated the enhanced function of QTRT1-containing eTGT in this process. This upregulation of QTRT1 in queuine-treated Caco2 BBE cells was also detected using IF staining (Figure 7H). As an important functional protein in cell permeability, alterations in  $\beta$ -catenin and claudin-5 were evaluated in queuine-treated Caco2 BBE cells. As shown in Figure 6F, the mRNA expression of  $\beta$ -catenin ( $P = .05$ ) and claudin-5 ( $P = .05$ ) was significantly upregulated after treating the cells with queuine compared with untreated cells. Similarly, these alterations were further verified by Western blot (Figure 7G) and IF staining (Figure 7H). There was no fluorescence staining in the IgG negative control used in the whole process of IF staining.

We used human colonoids to further investigate the benefits of queuine treatment. After treating the colonoids for 96 hours, the relative organoid volume size was significantly increased in the treated group compared with the control group ( $P = .05$ ) (Figure 8A). These findings clearly showed the functional role of queuine in alterations of intestinal cell proliferation. However, more studies need to be performed to investigate the potential underlying mechanisms. Taken together, these results clearly showed the importance of queuine and QTRT1 in cell proliferation and cell permeability, suggesting the potential treatment strategy for IBD patients using queuine or queuine-related compounds.

### Queuine Can Protect the Cells From DSS-Induced Inflammation on Organoids

We further investigated the protective effect of queuine against inflammation using organoids treated with DSS. The inflammation was induced by the DSS treatment as indicated by the upregulation of claudin-2 ( $P = .0001$ ) and the downregulation of claudin-5 ( $P = .05$ ) and  $\beta$ -catenin ( $P = .01$ ) (Figure 8B). Queuine treatment could protect the DSS-induced inflammation on organoids by altering expression of  $\beta$ -catenin and claudins (Figure 8B). These findings indicated the protective role of queuine in intestinal epithelial inflammation.

## Discussion

In the current study, we report that QTRT1 is significantly downregulated in human IBD patients, including UC and CD patients. In 2 IBD mouse models, the reduction in QTRT1 was significantly correlated with reduced cell proliferation and intestinal barrier function through altered claudin-2, claudin-5, and  $\beta$ -catenin. Queuine is capable of enhancing cell proliferation and intestinal barriers in cell cultures and human colonoids. Moreover, the downstream metabolite guanine of QTRT1 was involved in the process, and QTRT1-related tRNA synthesis was markedly altered in IBD patients.

Q-tRNA modification is critical for fidelity and accuracy when translating RNA to protein. Dysfunction of Q-tRNA is associated with cancer proliferation and malignancy.<sup>15,29,30</sup> However, the mechanisms by which Q and Q-tRNA modifications influence intestinal epithelial biology and chronic inflammation are unknown. For the first time, our study has demonstrated the downregulation of QTRT1 and Q-tRNA dysfunction in IBD. Furthermore, we provide evidence of altered downstream molecules, including guanine and the 4 tRNA synthetases, relevant to QTRT1 enzyme catalysis in human IBD. In eubacteria and eukaryotes, guanine is exchanged for queuine in tRNA isoacceptors containing a GUN sequence to obtain Q-tRNA, a reaction which is controlled by the eTGT enzyme, composing the QTRT1 and QTRT2 subunits.<sup>1,31</sup> Q-tRNA deficiency was found to be correlated with tumor growth, and leukemia.<sup>1,15,32,33</sup> Dysfunction of the eukaryotic tRNA-guanine transglycosylase complex, is reported to be involved in cancer proliferation and malignancy.<sup>15</sup> Our studies on tRNA regulation of  $\beta$ -catenin, a proliferation regulator, further supported the importance of Q-tRNA in health and disease.

We report that QTRT1 downregulation is related to altered  $\beta$ -catenin, claudin-2, and claudin-5. It is well known that TJs are essential to the function of the physical intestinal barrier by regulating the paracellular movement of various substances and waste across the intestinal epithelium. TJ dysfunction has been reported in IBD and other inflammatory diseases.<sup>34–36</sup> tRNA fulfills a critical link between protein synthesis and nucleic acid transcription.<sup>37</sup> It is reasonable to hypothesize that depletion in QTRT1 will impact Q-tRNA modification and further affect tRNA amino acid transferring activity. Thereafter, compromised tRNA activity would impact mRNA transcription and protein translation. The QTRT1 regulation of  $\beta$ -catenin and claudin-2/5 was further confirmed in cells with QTRT1 knockdown. On the one hand, QTRT1 knockout led to decreased protein levels of  $\beta$ -catenin and claudin-5 and increased claudin-2, suggesting decreased cell adhesion and increased permeability among cells. When the cells were treated with queuine, the substrate of the QTRT1-containing enzyme complex, the cell proliferation activity and claudin-5 expression were upregulated. The data indicate a novel role for QTRT1 in regulating intestinal epithelial cell junctions.

The sugar nucleotide queuosine is found within the anticodon loop of transfer RNA acceptors for the amino

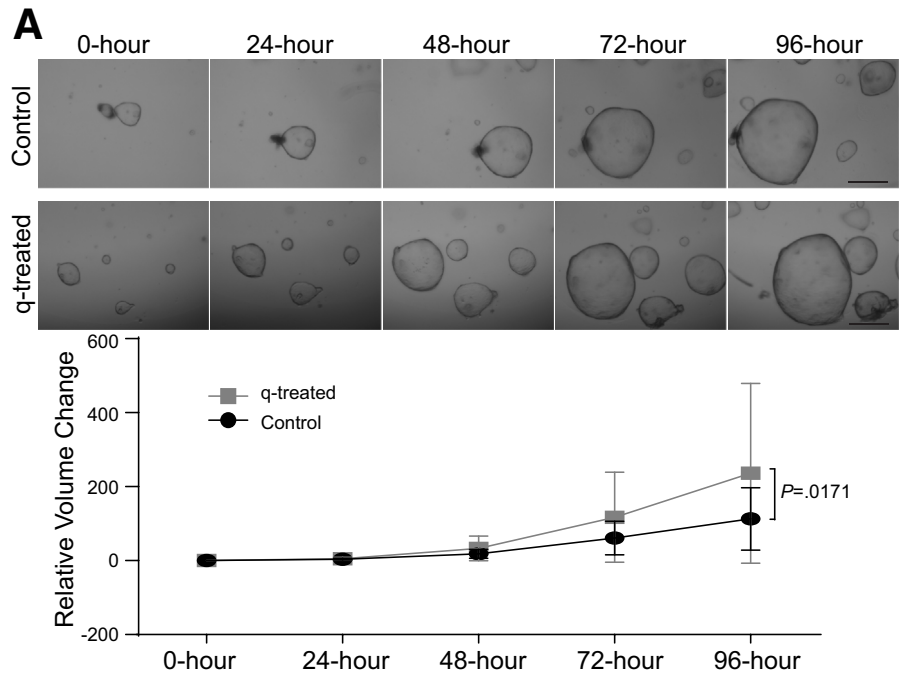
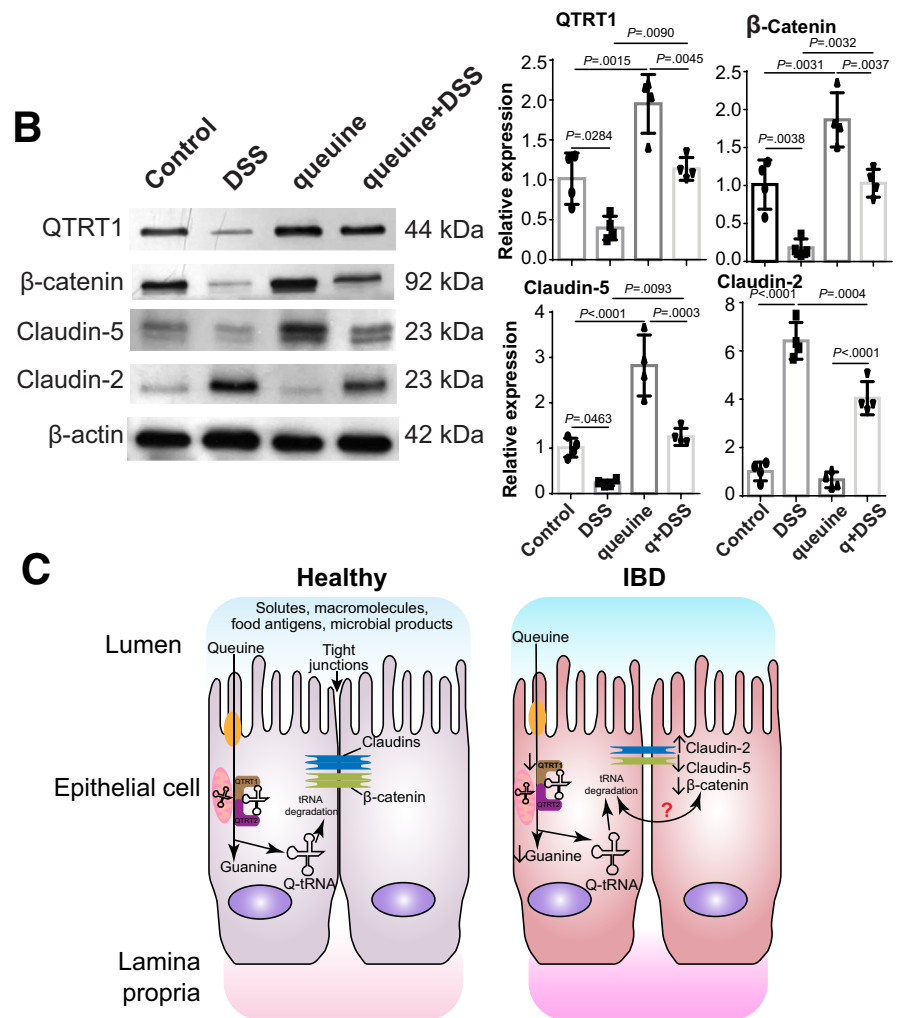


**Figure 8. Queuine treatment in human colonoids.** (A) Human colon organoids from healthy subjects were treated with queuine hydrochloride and monitored for 96 hours. The volume of the organoids was calculated with the formula:  $\text{volume } (\mu\text{m}^3) = [(4 \times \pi \times (\text{diameter}/2)^2)/3]$ . The scale bar is 750  $\mu\text{m}$ . Data are expressed as mean  $\pm$  SD, two-way analysis of variance.  $n = 10$  per group. (B) Mouse organoids were treated with DSS for 3 hours. Data are expressed as mean  $\pm$  SD, one-way analysis of variance.  $n = 4$  per group. (C) The working model of this study. Queuine base, and its corresponding nucleoside (queuosine), are produced by bacteria and salvaged by human body via the intestinal epithelium. Queuine replaces guanine at the wobble position of tRNAs and promotes efficient mRNA translation. Gut dysbiosis, one of the most common symptoms of the IBD patients, could critically impact on the functions of intestinal epithelium and queuine-to-guanine transportation, and mRNA translation. The protein expression of QTRT1, the catalytic subunit of the queuine-insertase complex, is suppressed in IBD patients. Reduced QTRT1 may lead to increased permeability and dysfunction of intestinal epithelial cells through modulating claudin-5 and  $\beta$ -catenin expression.



acids tyrosine, asparagine, aspartic acid, and histidine.<sup>1,31</sup> Our studies provide evidence that IBD patients have lower mRNA expression levels for these tRNA synthetases relative to healthy control subjects. We also found that the abundance of guanine was significantly lower in UC and CD patients. These findings reveal an alteration of QTRT1-related metabolites and tRNA synthetases in IBD patients, which highlight a critical role for QTRT1 in the biosynthesis of Q-tRNA and metabolites in related pathways.

Queuine is an elusive and less recognized micronutrient acquired from the diet or microbiome.<sup>1</sup> Micronutrients are essential elements needed by life in small quantities. They include microminerals and vitamins. Micronutrients from the diet and microbiota are essential to human health. Queuine is a microbiome/diet-derived chemical incorporated into the wobble position of tRNAs to affect fidelity and efficiency of translation from RNA to proteins. It is synthesized *de novo* in bacteria; mammals acquire queuine as micronutrient from their diet or intestinal microflora. Q-tRNA modification levels are highly dynamic and reflect the interplay between the host and microbiome. There is one article<sup>38</sup> that reported measured queuine in the plasma of neurologically healthy men and women (50–90 years of age). There was a decrease in queuine availability over aging, which was likely occurring in people with dysbiosis.<sup>38</sup> However, the queuine level in the patients with IBD is unknown. Understanding the cellular and organismal mechanisms of this microbiome-dependent micronutrient will advance the prevention of IBD and improve the quality of life of patients with IBD.

In summary, our data demonstrate that QTRT1 plays a novel role in human IBD by altering intestinal cell proliferation and junctions. Studies are needed to better understand human diseases caused by aberrations in tRNA modifications, also called tRNA modopathies.<sup>39</sup> The microbiome-dependent Q supply can be altered during disease or when a limited variety of food types are ingested. Investigations on gut tRNA modification in human IBD will uncover novel molecular mechanisms for potential disease prevention and therapy.

## Materials and Methods

### Reanalysis of Human IBD Datasets

For RNA expression analyses, we took advantage of microarray data reported in the GEO repository, using dataset GEO accession numbers GSE9452 and GSE83448, and normal ileum from control individuals. Four synthetases of tRNAs were compared between UC patients ( $n = 21$ ) and control subjects ( $n = 5$ ) sourced from GEO datasets (accession number GSE9452). Colonic mucosal samples were collected as endoscopic pinch biopsies from ulcerative colitis patients with and without macroscopic signs of inflammation.<sup>40</sup> CD patients were being operated on for intractable or complicated disease, undergoing an ileocolonic resection with ileocolonic anastomosis.<sup>20</sup> Similarly, the 4 synthetases of tRNAs (asparaginyl, aspartyl, histidyl, tyrosyl) were compared between CD patients ( $n = 36$ ) and control subjects ( $n = 32$ ) sourced from ArrayExpress (<https://www.ebi.ac.uk/arrayexpress>) with accession

number E-MTAB-5783. For metabolic compound analyses, we revisited the datasets available in Metabolomics Workbench. These 2 datasets were performed on both UC and CD patients (PR000639 with 145 UC patients, 266 CD patients, and 134 control subjects; PR000677 with 76 UC patients, 88 CD patients, and 56 control subjects).

### Animals and Animal Models

WT C57BL/6 and IL-10 knockout (IL-10<sup>-/-</sup>) mice were purchased from the Jackson Laboratory (Bar Harbor, ME). QTRT1 knockout mice have been described previously and maintained under approval of the Irish Health Products Regulatory Authority (AE19136/P086).<sup>3</sup> The mouse colitis model was induced by administering DSS, as previously described.<sup>41</sup> Experiments were performed on 8- to 12-week-old mice (both male and female). Animals were provided the same and consistent conditions and utilized in accordance with the UIC Animal Care Committee, the Office of Animal Care and Institutional Biosafety guidelines, and the animal protocol (number ACC 18-179).

Mouse colitis model was induced by administering the WT C57BL/6 mice (Jackson Laboratory) with 5% DSS (USB Corp, Cleveland, OH) dissolved in filter-purified and sterilized water *ad libitum* for 7 days, as previously described.<sup>41</sup>

IL-10 deficiency mouse colonic samples were harvest by scraping the tissue (intestinal epithelial cells) from the colon. The whole colon tissue from the DSS treated mice was used without scraping due to the severe damage of the intestine tissue. The collected cells or tissues were kept and sonicated in lysis buffer with 1% Triton X-100, 150 mM NaCl, 10 mM Tris, 1 mM EDTA, 1 mM EGTA, 0.2 mM sodium ortho-vanadate, and protease inhibitor cocktail, as previously described.<sup>41</sup> The protein concentration was measured using the Bio-Rad Reagent (Bio-Rad, Hercules, CA) according to the products' instruction. Finally, the protein was mixed with loading buffer (50 mM Tris, 100 mM dithiothreitol, 2% sodium dodecyl sulfate, 0.1% bromophenol blue, and 10% glycerol) and kept in the freezer until using for Western blot.

### QTRT1 Knockdown in Human Cells

The human HCT116 and Caco-2 BBE cells were cultured in 6-well tissue culture plates with Dulbecco's modified Eagle medium growth medium to 70%–80% confluence.<sup>42</sup> Subsequently, the cells were transfected with 2  $\mu$ g of QTRT1 double nickase plasmid (sc-413456-NIC) or control double nickase plasmid (sc-437281) (Santa Cruz Biotechnology, Dallas, TX), 10  $\mu$ L LTX Lipofectamine (Thermo Fisher Scientific, Rockford, IL), and 2.5  $\mu$ L PLUS Reagent (Invitrogen, San Diego, CA) per well (manufacturer's protocol). A QTRT1 double nickase plasmid-derived green fluorescent protein marker was used for positive selection of transfected cells through flow cytometry with a MoFlo Astrios cell sorter (Beckman Coulter, Indianapolis, IN).

### Western Blot Analysis

Animal intestinal epithelial tissue was lysed in lysis buffer as described previously. The Western blot analysis was performed as described previously.<sup>15,42</sup>

Cultured cells were rinsed twice in ice-cold Hanks' balanced salt solution (Sigma-Aldrich, St Louis, MO) and lysed in protein loading buffer then followed by sonication (Branson Sonifier, Danbury, CT) and centrifugation.<sup>15,42</sup> The target proteins were detected by special primary antibody (1:1000) followed by secondary antibody conjugated to horseradish peroxidase at 1:5000 dilution. The blots were visualized by ECL chemiluminescence (Thermo Fisher Scientific). All experiments were performed 3–5 times. Western blot bands were quantified using image analyzer (ImageJ 1.53c; National Institutes of Health, Bethesda, MD). The QTRT1 and Villin monoclonal antibody was purchased from Santa Cruz Biotechnology. Monoclonal antibodies of  $\beta$ -catenin from BD Transduction (San Jose, CA) and  $\beta$ -actin from Sigma-Aldrich were used in this study. Claudin-5, claudin-2 and claudin-7 monoclonal antibodies were purchased from Thermo Fisher Scientific. All chemicals were purchased from Sigma-Aldrich unless otherwise stated.

### IHC Staining

Human colon tissues from CD and UC patients and control subjects from non-IBD patients on paraffin-embedded sections (4  $\mu$ m) from our previous studies were used in this study.<sup>43,44</sup> IHC was performed on these paraffin-embedded sections.<sup>43–45</sup> Briefly, the paraffin sections were baked in an oven at 56°C for 30 minutes. The slides were deparaffinized and rehydrated in xylene, followed by graded ethanol washes at room temperature. Antigen retrieval was achieved by boiling the slides with sodium citrate buffer (0.01 M, pH 6.0). Sides were then incubated in hydrogen peroxide (3% H<sub>2</sub>O<sub>2</sub> in phosphate-buffered saline) for 10 minutes at room temperature, followed by incubation in 5% fetal bovine serum/phosphate-buffered saline for 1 hour. After that, the slides were incubated at 4°C with primary antibody at 1:100 dilution overnight. The sections were then incubated with secondary antibodies (Jackson ImmunoResearch, West Grove, PA) for 1 hour at room temperature,

**Table 1.** Methods Key Resources Table

Items	Company	Source
<b>Antibodies</b>		
$\beta$ -actin	Sigma-Aldrich	Cat. #: A5316
Alexa Fluor 488 donkey anti-mouse IgG	Invitrogen	Cat. #: A32766
Alexa Fluor 594 donkey anti-rabbit IgG	Invitrogen	Cat. #: A32740
Claudin 2	Invitrogen	Cat. #: 32-5600
Claudin 5	Invitrogen	Cat. #: 35-2500
Phospho-NF- $\kappa$ B p65 (Ser276)	Cell Signaling Technology	Cat. #: 3037
Purified Mouse Anti- NF- $\kappa$ B p65	BD Biosciences	Cat. #: 610869
Phospho- $\beta$ -Catenin (Ser33/37/Thr41)	Cell Signaling Technology	Cat. #: 9561
$\beta$ -Catenin	BD Biosciences	Cat. #: 610154
PCNA	Santa Cruz Biotechnology	Cat. #: sc-25280
Villin	Santa Cruz Biotechnology	Cat. #: sc-58897
QTRT1	Santa Cruz Biotechnology	Cat. #: sc-398918
<b>Chemicals</b>		
Fetal bovine serum	GIBCO	Cat. #: 16000044
DMEM	Corning	Cat. #: MT10013CV
DPBS	Corning	Cat. #: MT21031CV
Penicillin-streptomycin	Corning	Cat. #: MT30002CI
TRIzol	Thermo Fisher Scientific	Cat. #: 15596026
iScript cDNA synthesis kit	Bio-Rad	Cat. #: 1708840
SYBR Green PCR kit	Bio-Rad	Cat. #: 1708880
Triton X-100	Fisher BioReagents	Cat. #: BP151-100
16% Formaldehyde	Fisher BioReagents	Cat. #: 28908
DAPI	Invitrogen	Cat. #: D21490
Pierce™ ECL Western Blotting Substrate	Thermo Fisher Scientific	Cat. #: 32106
Queuine Hydrochloride	Santa Cruz Biotechnology	Cat. #: sc-394021
Dextran sulfate sodium salt	MP Biomedicals	Cat. #: 160110
Vybrant MTT Cell Proliferation Assay Kit	Molecular Probes	Cat. #: V13154
Recombinant Mouse TNF- $\alpha$	R&D Systems	Cat. #: 410-MT
<b>Software and algorithms</b>		
FlowJo Version 10.3	TreeStar	www.flowjo.com/
Microsoft Excel Version 16.24	Office 365	www.office.com/
Prism Version 8.1.1	GraphPad Software	www.graphpad.com/
Zeiss LSM710 confocal microscope	Carl Zeiss	N/A
EVOS M5000 Imaging System	Thermo Fisher Scientific	www.thermofisher.com
EVOM3	World Precision Instruments	www.wpi-europe.com
Nanodrop 2000	Thermo Fisher Scientific	N/A

TNF- $\alpha$ , tumor necrosis factor  $\alpha$ .

and VECTASTAIN ABC Kit (Vector Laboratories, Burlingame, CA) for 1 hour at room temperature. After that, the tissue sections were stained with DAB Substrate Kit (Vector Laboratories) and hematoxylin (Leica Biosystems, Buffalo Grove, IL) and examined with confocal microscope or EVOS M5000 (Thermo Fisher Scientific). The target cells were stained with QTRT1 monoclonal antibody (Santa Cruz Biotechnology). The IgG antibody protein (Jackson ImmunoResearch) was used as negative control for all the IHC staining experiments. The semi-quantitative analysis of IHC staining was performed using software ImageJ Fiji as described previously.<sup>45</sup>

### IF Staining

Fresh intestinal tissue was fixed in 10% neutral buffered formalin followed by paraffin embedding. Paraffin-embedded slides (4  $\mu\text{m}$ ) were prepared with a microtome.<sup>46</sup> The QTRT1 monoclonal antibody was purchased from Santa Cruz Biotechnology; claudin-2, -5, and -7 from Thermo Fisher Scientific; and  $\beta$ -catenin from BD Transduction (see detailed information in Table 1). The IgG antibody protein (Jackson ImmunoResearch) was used as a negative control for all IF staining experiments. The fluorescence intensity was evaluated with ImageJ.<sup>47</sup>

### Real-Time Quantitative PCR

Total RNA was extracted from cultured cell monolayers or tissues from the mice using TRIzol reagent (Thermo Fisher Scientific) by following the products' instruction. The total RNA from DSS-treated murine tissue was further purified via lithium chloride precipitation as described previously.<sup>48</sup> RNA reverse transcription was performed using the iScript complementary DNA synthesis kit (Bio-Rad) according to the manufacturer's directions. Then, the reverse-transcription complementary DNA reaction products were subjected to quantitative real-time PCR using the iTaq Universal SYBR green supermix (Bio-Rad) and primers from Primer Bank (Cambridge, MA) (Table 2) with the MyiQ single-color real-time PCR detection system (Bio-Rad). All expression levels were normalized to  $\beta$ -actin levels of the same sample. The percentage expression was calculated as the ratio of the normalized value of each sample to that of the corresponding untreated control cells.<sup>49</sup>

### Queuine Treatment of Cells and Human Colonoids

Caco-2 BBE cells were plated in triplicate at a density of  $1 \times 10^4$  cells per well in a 12-well culture plate. After 24 hours of culture, queuine hydrochloride (Toronto Research Chemicals, Toronto, Canada) was added to each well at a final concentration of 5  $\mu\text{M}$  for 24, 48, and 72 hours. Human colonoids from healthy people were prepared and maintained in Matrigel as described previously.<sup>50</sup> At day 6 after passage, the colonoids were treated with 5  $\mu\text{M}$  queuine hydrochloride and monitored by EVOS M5000 (Thermo Fisher Scientific). The diameter was measured by ImageJ, and the volume of the organoids was calculated with the formula:  $\text{volume} (\mu\text{m}^3) = [(4 \times \pi \times (\text{diameter}/2)^2)/3]$ .

**Table 2.** Real-Time PCR Primers Used

Primer	Nucleotides (5' – 3')
Human QTRT1 forward	5'-GAA GGG CAT CAC GAC CGA A-3'
Human QTRT1 reverse	5'-CCC GGC CTT AGA CCC AGA T-3'
Human $\beta$ -catenin forward	5'-AAA ATG GCA GTG CGT TTA G-3'
Human $\beta$ -catenin reverse	5'-TTT GAA GGC AGT CTG TCG TA-3'
Human claudin-5 forward	5'-GTT TTA CGA CCC GTC TGT GC-3'
Human claudin-5 reverse	5'-AGT GGC AGG AGA AGG TCA GC-3'
Human claudin-2 forward	5'-ACC TGC TAC CGC CAC TCT GT-3'
Human claudin-2 reverse	5'-CTC CCT GGC CTG CAT TAT CTC-3'
Human PCNA forward	5'-CCTGCTGGGATATTAGCTCCA-3'
Human PCNA reverse	5'-CAGCGGTAGGTGTCGAAGC-3'
Human $\beta$ -actin forward	5'-CAT GTA CGT TGC TAT CCA GGC-3'
Human $\beta$ -actin reverse	5'-CTC CTT AAT GTC ACG CAC GAT-3'
Mouse QTRT1 forward	5'-AAT TGG CCC CAC AAT CTG CT-3'
Mouse QTRT1 reverse	5'-CTG GGC TCA AAA GTG TCT CTT C-3'
Mouse $\beta$ -catenin forward	5'-TGC TGA AGG TGC TGT CTG TC-3'
Mouse $\beta$ -catenin reverse	5'-CTG CTT AGT CGC TGC ATC TG-3'
Mouse claudin-5 forward	5'-AGG CAC GGG TAG CAC TCA CG-3'
Mouse claudin-5 reverse	5'-CAT AGT TCT TCT TGT CGT AAT C-3'
Mouse claudin-2 forward	5'-GCA AAC AGG CTC CGA AGA TAC T-3'
Mouse claudin-2 reverse	5'-GAG ATG ATG CCC AAG TAC AGA G-3'
Mouse PCNA forward	5'-TTT GAG GCA CGC CTG ATC C-3'
Mouse PCNA reverse	5'-GGA GAC GTG AGA CGA GTC CAT-3'
Mouse $\beta$ -actin forward	5'-TGT TAC CAA CTG GGA CGA CA-3'
Mouse $\beta$ -actin reverse	5'-CTG GGT CAT CTT TTC ACG GT-3'

PCNA, proliferating cell nuclear antigen; PCR, polymerase chain reaction.

### TEER Assay

The HT-29 cells in complete media were seeded onto the 24-transwell plate at  $2.5 \times 10^5$  cells/200  $\mu\text{L}$ .<sup>51</sup> After 10 days of seeding, the cells were treated with 5  $\mu\text{M}$  queuine



hydrochloride, and the TEER was measured and monitored with EVOM3 (World Precision Instruments, Sarasota, FL) to test cell permeability.

### DSS Treatment of Mouse Organoids

Mouse intestine organoids were prepared and maintained as we described previously.<sup>50</sup> When the cells were ready, DSS was added to the cells at a final concentration of 200  $\mu$ M for 3 hours. In the queuine-treated group, the cells were treated with 5  $\mu$ M queuine final for 72 hours before DSS treatment.

### Statistical Analysis

Data shown in the bar figures are the average values from at least 3 independent experiments with mean  $\pm$  SD. All statistical tests were 2-sided. A *P* value  $<.05$  was considered statistically significant. The Spearman correlation coefficient test was used to analyze the correlation between 2 variables (protein expression) using the Hmisc package.<sup>52</sup> In the MTT assay, which was tested with generalized linear mixed models, Welch's *t* test was performed for the 24-hour and 48-hour analyses, while the Wilcoxon rank sum test was performed for the 72-hour analysis. The statistical analyses were conducted by GraphPad Prism 5 (GraphPad Software, San Diego, CA).

## References

1. Fergus C, Barnes D, Alqasem MA, et al. The queuine micronutrient: charting a course from microbe to man. *Nutrients* 2015;7:2897–2929.
2. Tuorto F, Lyko F. Genome recoding by tRNA modifications. *Open Biol* 2016;6:160287.
3. Rakovich T, Boland C, Bernstein I, et al. Queuosine deficiency in eukaryotes compromises tyrosine production through increased tetrahydrobiopterin oxidation. *J Biol Chem* 2011;286:19354–19363.
4. Katze JR, Basile B, McCloskey JA. Queuine, a modified base incorporated posttranscriptionally into eukaryotic transfer RNA: wide distribution in nature. *Science* 1982; 216:55–56.
5. Suzuki T, Yashiro Y, Kikuchi I, et al. Complete chemical structures of human mitochondrial tRNAs. *Nat Commun* 2020;11:4269.
6. Kersten H. The nutrient factor queuine: biosynthesis, occurrence in transfer RNA and function. *Biofactors* 1988;1:27–29.
7. Tuorto F, Legrand C, Cirzi C, et al. Queuosine-modified tRNAs confer nutritional control of protein translation. *EMBO J* 2018;37:e99777.
8. Torres AG, Batlle E, Ribas de Pouplana L. Role of tRNA modifications in human diseases. *Trends Mol Med* 2014; 20:306–314.
9. Zaborske JM, DuMont VL, Wallace EW, et al. A nutrient-driven tRNA modification alters translational fidelity and genome-wide protein coding across an animal genus. *PLoS Biol* 2014;12:e1002015.
10. Rivera-Nieves J, Bamias G, Vidrich A, et al. Emergence of perianal fistulizing disease in the SAMP1/YitFc mouse, a spontaneous model of chronic ileitis. *Gastroenterology* 2003;124:972–982.
11. Kellermayer R. Epigenetics and the developmental origins of inflammatory bowel diseases. *Can J Gastroenterol* 2012;26:909–915.
12. Xu J, Xu H-M, Yang M-F, et al. New insights into the epigenetic regulation of inflammatory bowel disease. *Front Pharmacol* 2022;13:813659.
13. Barnett M, Bermingham E, McNabb W, et al. Investigating micronutrients and epigenetic mechanisms in relation to inflammatory bowel disease. *Mutat Res* 2010; 690:71–80.
14. Matsunaga T, Iyoda T, Fukai F. Adhesion-dependent cell regulation via adhesion molecule, integrin: therapeutic application of integrin activation-modulating factors. In: Ohshima H, Makino K, eds. *Colloid and Interface Science in Pharmaceutical Research and Development*. New York: Elsevier, 2014:243–260.
15. Zhang J, Lu R, Zhang Y, et al. tRNA queuosine modification enzyme modulates the growth and microbiome recruitment to breast tumors. *Cancers (Basel)* 2020; 12:628.
16. Weber CR, Nalle SC, Tretiakova M, et al. Claudin-1 and claudin-2 expression is elevated in inflammatory bowel disease and may contribute to early neoplastic transformation. *Lab Invest* 2008;88:1110–1120.
17. Zeissig S, Bürgel N, Günzel D, et al. Changes in expression and distribution of claudin 2, 5 and 8 lead to discontinuous tight junctions and barrier dysfunction in active Crohn's disease. *Gut* 2007;56:61–72.
18. Zhu L, Han J, Li L, et al. Claudin family participates in the pathogenesis of inflammatory bowel diseases and colitis-associated colorectal cancer. *Front Immunol* 2019;10:1441.
19. Olsen J, Nielsen OH, Csillag C, Seidelin J. Definition of an ulcerative colitis preinflammatory state. *Gene Expression Omnibus*. Available at: <https://www.ncbi.nlm.nih.gov/geo/query/acc.cgi?acc=GSE9452>. Accessed January 23 2021.
20. Zabana Y, Loren V, Domenech E, et al. Transcriptomic identification of TMIGD1 and its relationship with the ileal epithelial cell differentiation in Crohn's disease. *Am J Physiol Gastrointest Liver Physiol* 2020; 319:G109–G120.
21. Kühn R, Löhler J, Rennick D, et al. Interleukin-10-deficient mice develop chronic enterocolitis. *Cell* 1993; 75:263–274.
22. Keubler LM, Buettner M, Häger C, et al. A multihit model: colitis lessons from the interleukin-10-deficient mouse. *Inflamm Bowel Dis* 2015;21:1967–1975.
23. Bleich A, Mähler M, Most C, et al. Refined histopathologic scoring system improves power to detect colitis QTL in mice. *Mamm Genome* 2004;15:865–871.
24. Valenta T, Hausmann G, Basler K. The many faces and functions of  $\beta$ -catenin. *EMBO J* 2012;31:2714–2736.
25. Zihni C, Mills C, Matter K, et al. Tight junctions: from simple barriers to multifunctional molecular gates. *Nat Rev Mol Cell Biol* 2016;17:564–580.

26. Global Burden of Disease Long COVID Collaborators, Wulf Hanson S, Abbafati C, Aerts JG, et al. Estimated global proportions of individuals with persistent fatigue, cognitive, and respiratory symptom clusters following symptomatic COVID-19 in 2020 and 2021. *JAMA* 2022; 328:1604–1615.
27. Dennis C, KP, Bullock K, et al. Longitudinal multiomics of the human microbiome in inflammatory bowel disease. *Metabolomics Workbench*. Available at: <https://www.metabolomicsworkbench.org/data/DRCCMetadata.php?Mode=Study&StudyID=ST000923&StudyType=MS&ResultType=1>. Accessed March 3, 2020.
28. Franzosa EA, Sirota-Madi A, Avila-Pacheco J, et al. Gut microbiome structure and metabolic activity in inflammatory bowel disease. *Nat Microbiol* 2019; 4:293–305.
29. Bai R, Sun D, Chen M, et al. Myeloid cells protect intestinal epithelial barrier integrity through the angiogenin/plexin-B2 axis. *EMBO J* 2020;39:e103325.
30. Chen Y, Shen J. Mucosal immunity and tRNA, tRF, and tiRNA. *J Mol Med (Berl)* 2021;99:47–56.
31. Yuan Y, Zallot R, Grove TL, et al. Discovery of novel bacterial queuine salvage enzymes and pathways in human pathogens. *Proc Natl Acad Sci U S A* 2019;116:19126–19135.
32. Ishiwata S, Katayama J, Shindo H, et al. Increased expression of queuosine synthesizing enzyme, tRNA-guanine transglycosylase, and queuosine levels in tRNA of leukemic cells. *J Biochem* 2001;129:13–17.
33. Varghese S, Cotter M, Chevot F, et al. In vivo modification of tRNA with an artificial nucleobase leads to full disease remission in an animal model of multiple sclerosis. *Nucleic Acids Res* 2017;45:2029–2039.
34. Bhat AA, Uppada S, Achkar IW, et al. Tight junction proteins and signaling pathways in cancer and inflammation: a functional crosstalk. *Front Physiol* 2018; 9:1942.
35. Landy J, Ronde E, English N, et al. Tight junctions in inflammatory bowel diseases and inflammatory bowel disease associated colorectal cancer. *World J Gastroenterol* 2016;22:3117–3126.
36. Lee B, Moon KM, Kim CY. Tight junction in the intestinal epithelium: its association with diseases and regulation by phytochemicals. *J Immunol Res* 2018;2018: 2645465.
37. de Farias ST, José MV. Transfer RNA: The molecular demiurge in the origin of biological systems. *Prog Biophys Mol Biol* 2020;153:28–34.
38. Richard P, Kozłowski L, Guillorit H, et al. Queuine, a bacterial-derived hypermodified nucleobase, shows protection in in vitro models of neurodegeneration. *PLoS One* 2021;16:e0253216.
39. Chujo T, Tomizawa K. Human transfer RNA modifications: diseases caused by aberrations in transfer RNA modifications. *FEBS J* 2021;288:7096–7122.
40. Olsen J, Gerds TA, Seidelin JB, et al. Diagnosis of ulcerative colitis before onset of inflammation by multivariate modeling of genome-wide gene expression data. *Inflamm Bowel Dis* 2009;15:1032–1038.
41. Wu S, Zhang Y-g, Lu R, et al. Intestinal epithelial vitamin D receptor deletion leads to defective autophagy in colitis. *Gut* 2015;64:1082–1094.
42. Zhang YG, Wu S, Lu R, et al. Tight junction CLDN2 gene is a direct target of the vitamin D receptor. *Sci Rep* 2015; 5:10642.
43. Zhang YG, Zhu X, Lu R, et al. Intestinal epithelial HMGB1 inhibits bacterial infection via STAT3 regulation of autophagy. *Autophagy* 2019;15:1935–1953.
44. Lu R, Zhang YG, Xia Y, et al. Paneth cell alertness to pathogens maintained by vitamin D receptors. *Gastroenterology* 2021;160:1269–1283.
45. Crowe AR, Yue W. Semi-quantitative determination of protein expression using immunohistochemistry staining and analysis: an integrated protocol. *Bio Protoc* 2019; 9:e3465.
46. Blikslager AT, Moeser AJ, Gookin JL, et al. Restoration of barrier function in injured intestinal mucosa. *Physiol Rev* 2007;87:545–564.
47. Keith R. Porter Imaging Facility. Determining fluorescence intensity and signal. Volume 2021. Available at: <https://kpif.umbc.edu/image-processing-resources/image-fiji/determining-fluorescence-intensity-and-positive-signal/>. Accessed July 28, 2021.
48. Viennois E, Tahsin A, Merlin D. Purification of total RNA from DSS-treated murine tissue via lithium chloride precipitation. *Bio Protoc* 2018;8:e2829.
49. Zhang YG, Lu R, Wu S, et al. Vitamin D receptor protects against dysbiosis and tumorigenesis via the JAK/STAT pathway in intestine. *Cell Mol Gastroenterol Hepatol* 2020;10:729–746.
50. Zhang YG, Sun J. Study bacteria-host interactions using intestinal organoids. *Methods Mol Biol* 2019; 1576:249–254.
51. Chatterjee I, Zhang Y, Zhang J, et al. Overexpression of vitamin D receptor in intestinal epithelia protects against colitis via upregulating tight junction protein claudin 15. *J Crohns Colitis* 2021;15:1720–1736.
52. Harrell FE Jr. wcfCDamo. Hmisc: Harrell Miscellaneous. Available at: <https://rdrr.io/cran/Hmisc/>. Accessed May 8 2020.

---

Received July 11, 2022. Accepted February 8, 2023.

#### Correspondence

Address correspondence to: Jun Sun, PhD, Division of Gastroenterology and Hepatology, Department of Medicine, University of Illinois Chicago, 840 S Wood Street, Room 704 CSB, MC716, Chicago, Illinois, 60612. e-mail: [junsun7@uic.edu](mailto:junsun7@uic.edu).

#### CRedit Authorship Contributions

Jilei Zhang, PhD (Data curation: Lead; Formal analysis: Lead; Investigation: Lead; Methodology: Lead; Resources: Supporting; Software: Equal; Validation: Equal; Visualization: Lead; Writing – original draft: Lead; Writing – review & editing: Equal)

Yong-Guo Zhang, PhD (Data curation: Equal; Formal analysis: Supporting; Investigation: Supporting; Methodology: Supporting; Validation: Supporting; Visualization: Supporting; Writing – review & editing: Equal)

Callum J McGrenaghan, PhD (Resources: Supporting; Writing – review & editing: Supporting)

Vincent P Kelly P Kelly, PhD (Resources: Supporting; Writing – review & editing: Supporting)

Yinglin Xia, PhD (Data curation: Equal; Formal analysis: Equal; Methodology: Equal; Software: Supporting; Validation: Supporting; Visualization: Supporting; Writing – review & editing: Equal)

Jun Sun, PhD (Conceptualization: Lead; Data curation: Supporting; Formal analysis: Equal; Funding acquisition: Lead; Investigation: Equal; Methodology: Supporting; Project administration: Lead; Resources: Lead; Software: Supporting; Supervision: Lead; Validation: Equal; Visualization: Supporting; Writing – original draft: Lead; Writing – review & editing: Lead)

#### **Conflicts of Interest**

The authors disclose no conflicts.

#### **Funding**

This project was supported by the Crohn's and Colitis Foundation Senior Research Award (Award Number 902766 to Jun Sun); the National Institute of Diabetes and Digestive and Kidney Diseases (R01DK105118-01 and R01DK114126 to Jun Sun); U.S. Department of Defense Congressionally Directed Medical Research Programs (BC191198 to Jun Sun); VA Merit Award BX-19-00 (to Jun Sun); and a US-Ireland R&D Partnership grant supported by the Health Research Board, Science Foundation Ireland, and the National Institute of Health (USIRL-2019-2 to Vincent P. Kelly). The contents do not represent the views of the U.S. Department of Veterans Affairs or the U.S. Government. The study sponsor played no role in the study design in the collection, analysis, and interpretation of data.